Chapter 6
Conical Shells

Conical shells are another special type of shells of revolution. The middle surface of a conical shell is generated by revolving a straight line (generator line) around an axis that is not paralleled to the line itself. Conical shells can have different geometrical shapes. This chapter is organizationally limited to conical shells (both the closed shells and the open ones) having circular cross-sections. In this type of conical shells, the generator line rotates about a fixed axis and results in a constant vertex half-angle angle (φ) with respect to the axis. Specially, the vertex half-angle angle may be equal to zero or 90° ($\pi/2$). In the first case, the cylindrical shells discussed in Chap. 5 will be obtained. Thus, cylindrical shells can be viewed as a special type of the conical shells, and conical shells have all the classifying parameters of the cylindrical shells (Leissa 1973). For the second case, the generator line is vertical to the axis, and the special case of circular plates is obtained.

Laminated conical shells are also one of the important structural components which are widely used in naval vessels, missiles, spacecrafts and other cutting-edge engineering fields. The vibration analysis of them is often required and has always been one important research subject in these fields (Civalek 2006, 2007, 2013; Lam et al. 2002; Ng et al. 2003; Shu 1996; Tong 1993, 1994a, b; Tornabene 2011; Viswanathan et al. 2012; Wu and Lee 2011; Wu and Wu 2000). However, comparing with the cylindrical shells and the circular plates, relatively little literature is available regarding the conical shells due to the fact that the conical coordinate system is function of the meridional direction and the equations of motion for conical shells consist of a set of partial differential equations with variable coefficients.

This chapter is focused on vibration analysis of laminated conical shells with general boundary conditions. Equations of conical shells on the basis of the classical shell theory (CST) and the shear deformation shell theory (SDST) are presented in the first and second sections, respectively, by substituting the proper Lamé parameters of conical shells in the general shell equations (see Chap. 1). Then, in the framework of SDST, numerous vibration results of laminated closed and open conical shells with different boundary conditions, lamination schemes and geometry parameters are given in the third and fourth sections by using the modified Fourier series and the weak form solution procedure.

G. Jin et al., *Structural Vibration*, DOI 10.1007/978-3-662-46364-2_6

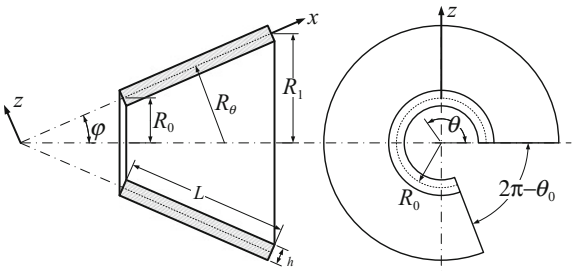

Fig. 6.1 Geometry notations and coordinate system of conical shells

As shown in Fig. 6.1, a general laminated open conical shell with length L, vertex half-angle angle φ, total thickness h, circumferential included angle θ_0, small edge radius R_0 and large edge radius R_1 is selected as the analysis model. The middle surface of the conical shell where an orthogonal coordinate system (x, θ and z) is fixed is taken as the reference surface, in which the x co-ordinate is measured along the generator of the cone starting at the vertex and the θ and z co-ordinates are taken in the circumferential and radial directions, respectively. The middle surface displacements of the conical shell in the x, θ and z directions are denoted by u, v and w, respectively. The conical shell is assumed to be composed of arbitrary number of liner orthotropic laminas which are bonded together rigidly. The mean radius of the conical shell at any point x along its length can be written as:

$$R = x \sin \varphi \tag{6.1}$$

Considering the conical shell in Fig. 6.1 and its conical coordinate system, the coordinates, characteristics of the Lamé parameters and radii of curvatures are:

$$\alpha = x, \quad \beta = \theta, \quad A = 1, \quad B = x \sin \varphi, \quad R_\alpha = \infty, \quad R_\beta = x \tan \varphi \tag{6.2}$$

6.1 Fundamental Equations of Thin Laminated Conical Shells

Closed conical shells can be defined as a special case of open conical shells having circumferential included angle of 2π (360°). We will first derive the fundamental equations for thin open conical shells. The equations are formulated for the general dynamic analysis by substituting Eq. (6.2) into the general classical shell equations developed in Sect. 1.2. It can be readily specialized to the static and free vibration analysis.

6.1.1 Kinematic Relations

Substituting Eq. (6.2) into Eq. (1.7), the middle surface strains and curvature changes of conical shells can be specialized from those of general thin shells. They are formed in terms of the middle surface displacements as:

$$\begin{aligned}
&\varepsilon_x^0 = \frac{\partial u}{\partial x} && \chi_x = -\frac{\partial^2 w}{\partial x^2} \\
&\varepsilon_\theta^0 = \frac{\partial v}{xs\partial\theta} + \frac{u}{x} + \frac{w}{xt} && \chi_\theta = \frac{c\partial v}{x^2 s^2 \partial\theta} - \frac{\partial^2 w}{x^2 s^2 \partial\theta^2} - \frac{\partial w}{x\partial x} \\
&\gamma_{x\theta}^0 = \frac{\partial v}{\partial x} + \frac{\partial u}{xs\partial\theta} - \frac{v}{x} && \chi_{x\theta} = \frac{\partial v}{xt\partial x} - \frac{2v}{x^2 t} - \frac{2\partial^2 w}{xs\partial x\partial\theta} + \frac{2\partial w}{x^2 s\partial\theta} \\
&\text{and} \quad s = \sin\varphi && c = \cos\varphi \qquad t = \tan\varphi
\end{aligned} \tag{6.3}$$

where ε_x^0, ε_θ^0 and $\gamma_{x\theta}^0$ denote the normal and shear middle surface strains. χ_x, χ_θ and $\chi_{x\theta}$ are the corresponding curvature and twist changes. Then, the state of strain at an arbitrary point in the kth layer of a laminated conical shell can be written as:

$$\begin{aligned}
\varepsilon_x &= \varepsilon_x^0 + z\chi_x \\
\varepsilon_\theta &= \varepsilon_\theta^0 + z\chi_\theta \\
\gamma_{x\theta} &= \gamma_{x\theta}^0 + z\chi_{x\theta}
\end{aligned} \tag{6.4}$$

where Z_{k+1}<z < Z_k. And Z_{k+1} and Z_k denote the distances from the top surface and bottom surface of the layer to the referenced middle surface, respectively.

6.1.2 Stress-Strain Relations and Stress Resultants

For laminated conical shells made of composite layers, the well-known stress-strain relations are given as in Eq. (5.4). It should be noted that the materials considered in this chapter are restricted to conical orthotropy. Substituting Eq. (6.2) into Eq. (1.14), the force and moment resultants of the conical shell can be obtained in terms of the middle surface strains and curvature changes as

$$\begin{bmatrix} N_x \\ N_\theta \\ N_{x\theta} \\ M_x \\ M_\theta \\ M_{x\theta} \end{bmatrix} = \begin{bmatrix} A_{11} & A_{12} & A_{16} & B_{11} & B_{12} & B_{16} \\ A_{12} & A_{22} & A_{26} & B_{12} & B_{22} & B_{26} \\ A_{16} & A_{26} & A_{66} & B_{16} & B_{26} & B_{66} \\ B_{11} & B_{12} & B_{16} & D_{11} & D_{12} & D_{16} \\ B_{12} & B_{22} & B_{26} & D_{12} & D_{22} & D_{26} \\ B_{16} & B_{26} & B_{66} & D_{16} & D_{26} & D_{66} \end{bmatrix} \begin{bmatrix} \varepsilon_x^0 \\ \varepsilon_\theta^0 \\ \gamma_{x\theta}^0 \\ \chi_x \\ \chi_\theta \\ \chi_{x\theta} \end{bmatrix} \tag{6.5}$$

where N_x, N_θ and $N_{x\theta}$ are the normal and shear force resultants and M_x, M_θ and $M_{x\theta}$ denote the bending and twisting moment resultants. The stiffness coefficients A_{ij}, B_{ij}, and D_{ij} are written as in Eq. (1.15).

6.1.3 Energy Functions

The strain energy function of thin laminated conical shells during vibration can be written in terms of the middle surface strains, curvature changes and stress resultants as:

$$U_s = \frac{1}{2}\int_x \int_\theta \left\{ \begin{array}{l} N_x\varepsilon_x^0 + N_\theta\varepsilon_\theta^0 + N_{x\theta}\gamma_{x\theta}^0 \\ +M_x\chi_x + M_\theta\chi_\theta + M_{x\theta}\chi_{x\theta} \end{array} \right\} xsd\theta dx \tag{6.6}$$

Substituting Eqs. (6.3) and (6.5) into Eq. (6.6), the strain energy functions of the shells can be written in terms of middle surface displacements. The corresponding kinetic energy (T) of the conical shells during vibration can be written as:

$$T = \frac{1}{2}\int_x \int_\theta I_0 \left\{ \left(\frac{\partial u}{\partial t}\right)^2 + \left(\frac{\partial v}{\partial t}\right)^2 + \left(\frac{\partial w}{\partial t}\right)^2 \right\} xsd\theta dx \tag{6.7}$$

where the inertia term I_0 is the same as in Eq. (1.19). Suppose q_x, q_θ and q_z are the external loads in the x, θ and z directions, respectively. Thus, the external work can be expressed as:

$$W_e = \int_x \int_\theta \{q_x u + q_\theta v + q_z w\} R dx d\theta \tag{6.8}$$

The same as usual, the general boundary conditions of a conical shell are implemented by using the artificial spring boundary technique. Letting symbols k_ψ^u, k_ψ^v, k_ψ^w and K_ψ^w ($\psi = x_0$, θ_0, x_1 and θ_1) to indicate the stiffness of the boundary springs at the boundaries $R = R_0$, $\theta = 0$, $R = R_1$ and $\theta = \theta_0$, respectively, thus, the deformation strain energy stored in the boundary springs (U_{sp}) during vibration can be defined as:

$$\begin{aligned} U_{sp} = & \frac{1}{2}\int_\theta \left\{ \begin{array}{l} x\left[k_{x0}^u u^2 + k_{x0}^v v^2 + k_{x0}^w w^2 + K_{x0}^x(\partial w/\partial x)\right]|_{R=R_0} \\ +x\left[k_{x1}^u u^2 + k_{x1}^v v^2 + k_{x1}^w w^2 + K_{x1}^x(\partial w/\partial x)\right]|_{R=R_1} \end{array} \right\} sd\theta \\ & + \frac{1}{2}\int_x \left\{ \begin{array}{l} \left[k_{\theta 0}^u u^2 + k_{\theta 0}^v v^2 + k_{\theta 0}^w w^2 + K_{\theta 0}^x(\partial w/xs\partial\theta)\right]|_{\theta=0} \\ +\left[k_{\theta 1}^u u^2 + k_{\theta 1}^v v^2 + k_{\theta 1}^w w^2 + K_{\theta 1}^x(\partial w/xs\partial\theta)\right]|_{\theta=\theta_0} \end{array} \right\} dx \end{aligned} \tag{6.9}$$

6.1.4 Governing Equations and Boundary Conditions

Substituting Eq. (6.2) into Eq. (1.28) and then simplifying the expressions, the resulting governing equations for conical shells are:

$$\begin{aligned}
&\frac{\partial N_x}{\partial x}+\frac{N_x-N_\theta}{x}+\frac{\partial N_{x\theta}}{xs\partial\theta}+q_x=I_0\frac{\partial^2 u}{\partial t^2}\\
&\frac{\partial N_{x\theta}}{\partial x}+\frac{\partial N_\theta}{xs\partial\theta}+\frac{2N_{x\theta}}{x}+\frac{Q_\theta}{xt}+q_\theta=I_0\frac{\partial^2 v}{\partial t^2}\\
&-\frac{N_\theta}{xt}+\frac{\partial Q_x}{\partial x}+\frac{Q_x}{x}+\frac{\partial Q_\theta}{xs\partial\theta}+q_z=I_0\frac{\partial^2 w}{\partial t^2}
\end{aligned}\tag{6.10}$$

where Q_x and Q_θ are defined as

$$\begin{aligned}
Q_x&=\frac{\partial M_x}{\partial x}+\frac{\partial M_{x\theta}}{xs\partial\theta}+\frac{M_x-M_\theta}{x}\\
Q_\theta&=\frac{\partial M_\theta}{xs\partial\theta}+\frac{\partial M_{x\theta}}{\partial x}+\frac{2M_{x\theta}}{x}
\end{aligned}\tag{6.11}$$

Substituting Eqs. (6.3), (6.5) and (6.11) into Eq. (6.10) yields the governing equations in terms of displacements as:

$$\left(\begin{bmatrix}L_{11}&L_{12}&L_{13}\\L_{21}&L_{22}&L_{23}\\L_{31}&L_{32}&L_{33}\end{bmatrix}-\omega^2\begin{bmatrix}-I_0&0&0\\0&-I_0&0\\0&0&-I_0\end{bmatrix}\right)\begin{bmatrix}u\\v\\w\end{bmatrix}=\begin{bmatrix}-p_x\\-p_\theta\\-p_z\end{bmatrix}\tag{6.12}$$

The coefficients of the linear operator L_{ij} are written as

$$\begin{aligned}
L_{11}=&\frac{\partial}{\partial x}\left(A_{11}\frac{\partial}{\partial x}+\frac{A_{12}}{x}+\frac{A_{16}}{xs}\frac{\partial}{\partial\theta}\right)+\frac{1}{xs}\frac{\partial}{\partial\theta}\left(A_{16}\frac{\partial}{\partial x}+\frac{A_{26}}{x}+\frac{A_{66}}{xs}\frac{\partial}{\partial\theta}\right)\\
&+\frac{1}{x}\left((A_{11}-A_{12})\frac{\partial}{\partial x}+\frac{A_{12}-A_{22}}{x}+\frac{A_{16}-A_{26}}{xs}\frac{\partial}{\partial\theta}\right)\\
L_{12}=&\frac{\partial}{\partial x}\left(\frac{A_{12}}{xs}\frac{\partial}{\partial\theta}+A_{16}\left(\frac{\partial}{\partial x}-\frac{1}{x}\right)+\frac{B_{12}c}{x^2s^2}\frac{\partial}{\partial\theta}+\frac{B_{16}}{xt}\left(\frac{\partial}{\partial x}-\frac{2}{x}\right)\right)\\
&+\frac{1}{x}\left(\frac{A_{12}}{xs}\frac{\partial}{\partial\theta}+A_{16}\left(\frac{\partial}{\partial x}-\frac{1}{x}\right)+\frac{B_{12}c}{x^2s^2}\left(\frac{c\partial v}{x^2s^2\partial\theta}\right)+\frac{B_{16}}{xt}\left(\frac{\partial}{\partial x}-\frac{2}{x}\right)\right)\\
&-\frac{1}{x}\left(\frac{A_{22}}{xs}\frac{\partial}{\partial\theta}+A_{26}\left(\frac{\partial}{\partial x}-\frac{1}{x}\right)+\frac{B_{22}c}{x^2s^2}\left(\frac{c\partial v}{x^2s^2\partial\theta}\right)+\frac{B_{26}}{xt}\left(\frac{\partial}{\partial x}-\frac{2}{x}\right)\right)\\
&+\frac{1}{xs}\frac{\partial}{\partial\theta}\left(\frac{A_{26}}{xs}\frac{\partial}{\partial\theta}+A_{66}\left(\frac{\partial}{\partial x}-\frac{1}{x}\right)+\frac{B_{26}c}{x^2s^2}\frac{\partial}{\partial\theta}+\frac{B_{66}}{xt}\left(\frac{\partial}{\partial x}-\frac{2}{x}\right)\right)\\
L_{13}=&\frac{\partial}{\partial x}\left(\frac{A_{12}}{xt}-B_{11}\frac{\partial^2}{\partial x^2}-\frac{B_{12}}{x}\left(\frac{\partial^2}{xs^2\partial\theta^2}+\frac{\partial}{\partial x}\right)-\frac{2B_{16}}{xs}\left(\frac{\partial^2}{\partial x\partial\theta}-\frac{\partial}{x\partial\theta}\right)\right)\\
&+\frac{1}{x}\left(\frac{A_{12}}{xt}-B_{11}\frac{\partial^2}{\partial x^2}-\frac{B_{12}}{x}\left(\frac{\partial^2}{xs^2\partial\theta^2}+\frac{\partial}{\partial x}\right)-\frac{2B_{16}}{xs}\left(\frac{\partial^2}{\partial x\partial\theta}-\frac{\partial}{x\partial\theta}\right)\right)\\
&-\frac{1}{x}\left(\frac{A_{22}}{xt}-B_{12}\frac{\partial^2}{\partial x^2}-\frac{B_{22}}{x}\left(\frac{\partial^2}{xs^2\partial\theta^2}+\frac{\partial}{\partial x}\right)-\frac{2B_{26}}{xs}\left(\frac{\partial^2}{\partial x\partial\theta}-\frac{\partial}{x\partial\theta}\right)\right)\\
&+\frac{1}{xs}\frac{\partial}{\partial\theta}\left(\frac{A_{16}}{xt}-B_{16}\frac{\partial^2}{\partial x^2}-\frac{B_{26}}{x}\left(\frac{\partial^2}{xs^2\partial\theta^2}+\frac{\partial}{\partial x}\right)-\frac{2B_{66}}{xs}\left(\frac{\partial^2}{\partial x\partial\theta}-\frac{\partial}{x\partial\theta}\right)\right)
\end{aligned}$$

$$
\begin{aligned}
L_{21} = {} & \frac{\partial}{\partial x}\left(A_{16}\frac{\partial}{\partial x}+\frac{A_{26}}{x}+\frac{A_{66}}{xs}\frac{\partial}{\partial\theta}\right)+\frac{2}{x}\left(A_{16}\frac{\partial}{\partial x}+\frac{A_{26}}{x}+\frac{A_{66}}{xs}\frac{\partial}{\partial\theta}\right)\\
& +\frac{1}{xs}\frac{\partial}{\partial\theta}\left(A_{12}\frac{\partial}{\partial x}+\frac{A_{22}}{x}+\frac{A_{26}}{xs}\frac{\partial}{\partial\theta}\right)+\frac{c}{x^2s^2}\frac{\partial}{\partial\theta}\left(B_{12}\frac{\partial}{\partial x}+\frac{B_{22}}{x}+\frac{B_{26}}{xs}\frac{\partial}{\partial\theta}\right)\\
& +\frac{1}{xt}\frac{\partial}{\partial x}\left(B_{16}\frac{\partial}{\partial x}+\frac{B_{26}}{x}+\frac{B_{66}}{xs}\frac{\partial}{\partial\theta}\right)+\frac{2}{x^2t}\left(B_{16}\frac{\partial}{\partial x}+\frac{B_{26}}{x}+\frac{B_{66}}{xs}\frac{\partial}{\partial\theta}\right)\\
L_{22} = {} & \frac{\partial}{\partial x}\left(\frac{A_{26}}{xs}\frac{\partial}{\partial\theta}+A_{66}\left(\frac{\partial}{\partial x}-\frac{1}{x}\right)+\frac{B_{26}c}{x^2s^2}\frac{\partial}{\partial\theta}+\frac{B_{66}}{xt}\left(\frac{\partial}{\partial x}-\frac{2}{x}\right)\right)\\
& +\frac{2}{x}\left(\frac{A_{26}}{xs}\frac{\partial}{\partial\theta}+A_{66}\left(\frac{\partial}{\partial x}-\frac{1}{x}\right)+\frac{B_{26}c}{x^2s^2}\frac{\partial}{\partial\theta}+\frac{B_{66}}{xt}\left(\frac{\partial}{\partial x}-\frac{2}{x}\right)\right)\\
& +\frac{1}{xs}\frac{\partial}{\partial\theta}\left(\frac{A_{22}}{xs}\frac{\partial}{\partial\theta}+A_{26}\left(\frac{\partial}{\partial x}-\frac{1}{x}\right)+\frac{B_{22}c}{x^2s^2}\frac{\partial}{\partial\theta}+\frac{B_{26}}{xt}\left(\frac{\partial}{\partial x}-\frac{2}{x}\right)\right)\\
& +\frac{c}{x^2s^2}\frac{\partial}{\partial\theta}\left(\frac{B_{22}}{xs}\frac{\partial}{\partial\theta}+B_{26}\left(\frac{\partial}{\partial x}-\frac{1}{x}\right)+\frac{D_{22}c}{x^2s^2}\frac{\partial}{\partial\theta}+\frac{D_{26}}{xt}\left(\frac{\partial}{\partial x}-\frac{2}{x}\right)\right)\\
& +\frac{1}{xt}\frac{\partial}{\partial x}\left(\frac{B_{26}}{xs}\frac{\partial}{\partial\theta}+B_{66}\left(\frac{\partial}{\partial x}-\frac{1}{x}\right)+\frac{D_{26}c}{x^2s^2}\frac{\partial}{\partial\theta}+\frac{D_{66}}{xt}\left(\frac{\partial}{\partial x}-\frac{2}{x}\right)\right)\\
& +\frac{2}{x^2t}\left(\frac{B_{26}}{xs}\frac{\partial}{\partial\theta}+B_{66}\left(\frac{\partial}{\partial x}-\frac{1}{x}\right)+\frac{D_{26}c}{x^2s^2}\frac{\partial}{\partial\theta}+\frac{D_{66}}{xt}\left(\frac{\partial}{\partial x}-\frac{2}{x}\right)\right)\\
L_{23} = {} & \frac{\partial}{\partial x}\left(\frac{A_{26}}{xt}-B_{16}\frac{\partial^2}{\partial x^2}-\frac{B_{26}}{x}\left(\frac{\partial^2}{xs^2\partial\theta^2}+\frac{\partial}{\partial x}\right)-\frac{2B_{66}}{xs}\left(\frac{\partial^2}{\partial x\partial\theta}-\frac{\partial w}{x\partial\theta}\right)\right)\\
& +\frac{2}{x}\left(\frac{A_{26}}{xt}-B_{16}\frac{\partial^2}{\partial x^2}-\frac{B_{26}}{x}\left(\frac{\partial^2}{xs^2\partial\theta^2}+\frac{\partial}{\partial x}\right)-\frac{2B_{66}}{xs}\left(\frac{\partial^2}{\partial x\partial\theta}-\frac{\partial w}{x\partial\theta}\right)\right)\\
& +\frac{1}{xs}\frac{\partial}{\partial\theta}\left(\frac{A_{22}}{xt}-B_{12}\frac{\partial^2}{\partial x^2}-\frac{B_{22}}{x}\left(\frac{\partial^2}{xs^2\partial\theta^2}+\frac{\partial}{\partial x}\right)-\frac{2B_{26}}{xs}\left(\frac{\partial^2}{\partial x\partial\theta}-\frac{\partial w}{x\partial\theta}\right)\right)\\
& +\frac{c}{x^2s^2}\frac{\partial}{\partial\theta}\left(\frac{B_{22}}{xt}-D_{12}\frac{\partial^2}{\partial x^2}-\frac{D_{22}}{x}\left(\frac{\partial^2}{xs^2\partial\theta^2}+\frac{\partial}{\partial x}\right)-\frac{2D_{26}}{xs}\left(\frac{\partial^2}{\partial x\partial\theta}-\frac{\partial w}{x\partial\theta}\right)\right)\\
& +\frac{1}{xt}\frac{\partial}{\partial x}\left(\frac{B_{26}}{xt}-D_{16}\frac{\partial^2}{\partial x^2}-\frac{D_{26}}{x}\left(\frac{\partial^2}{xs^2\partial\theta^2}+\frac{\partial}{\partial x}\right)-\frac{2D_{66}}{xs}\left(\frac{\partial^2}{\partial x\partial\theta}-\frac{\partial w}{x\partial\theta}\right)\right)\\
& +\frac{2}{x^2t}\left(\frac{B_{26}}{xt}-D_{16}\frac{\partial^2}{\partial x^2}-\frac{D_{26}}{x}\left(\frac{\partial^2}{xs^2\partial\theta^2}+\frac{\partial}{\partial x}\right)-\frac{2D_{66}}{xs}\left(\frac{\partial^2}{\partial x\partial\theta}-\frac{\partial w}{x\partial\theta}\right)\right)
\end{aligned}
$$

$$
\begin{aligned}
L_{31} = {} & \frac{-1}{xt}\left(A_{12}\frac{\partial}{\partial x}+\frac{A_{22}}{x}+\frac{A_{26}}{xs}\frac{\partial}{\partial\theta}\right) \\
& +\frac{\partial}{\partial x}\begin{pmatrix}\frac{\partial}{\partial x}\left(B_{11}\frac{\partial}{\partial x}+\frac{B_{12}}{x}+\frac{B_{16}}{xs}\frac{\partial}{\partial\theta}\right)+\frac{1}{xs}\frac{\partial}{\partial\theta}\left(B_{16}\frac{\partial}{\partial x}+\frac{B_{26}}{x}+\frac{B_{66}}{xs}\frac{\partial}{\partial\theta}\right)\\ +\frac{1}{x}\left(B_{11}\frac{\partial}{\partial x}+\frac{B_{12}}{x}+\frac{B_{16}}{xs}\frac{\partial}{\partial\theta}\right)-\frac{1}{x}\left(B_{12}\frac{\partial}{\partial x}+\frac{B_{22}}{x}+\frac{B_{26}}{xs}\frac{\partial}{\partial\theta}\right)\end{pmatrix} \\
& +\frac{1}{x}\begin{pmatrix}\frac{\partial}{\partial x}\left(B_{11}\frac{\partial}{\partial x}+\frac{B_{12}}{x}+\frac{B_{16}}{xs}\frac{\partial}{\partial\theta}\right)+\frac{1}{xs}\frac{\partial}{\partial\theta}\left(B_{16}\frac{\partial}{\partial x}+\frac{B_{26}}{x}+\frac{B_{66}}{xs}\frac{\partial}{\partial\theta}\right)\\ +\frac{1}{x}\left(B_{11}\frac{\partial}{\partial x}+\frac{B_{12}}{x}+\frac{B_{16}}{xs}\frac{\partial}{\partial\theta}\right)-\frac{1}{x}\left(B_{12}\frac{\partial}{\partial x}+\frac{B_{22}}{x}+\frac{B_{26}}{xs}\frac{\partial}{\partial\theta}\right)\end{pmatrix} \\
& +\frac{1}{xs}\frac{\partial}{\partial\theta}\begin{pmatrix}\frac{1}{xs}\frac{\partial}{\partial\theta}\left(B_{12}\frac{\partial}{\partial x}+\frac{B_{22}}{x}+\frac{B_{26}}{xs}\right)+\frac{\partial}{\partial x}\left(B_{16}\frac{\partial}{\partial x}+\frac{B_{26}}{x}+\frac{B_{66}}{xs}\frac{\partial}{\partial\theta}\right)\\ +\frac{2}{x}\left(B_{16}\frac{\partial}{\partial x}+\frac{B_{26}}{x}+\frac{B_{66}}{xs}\frac{\partial}{\partial\theta}\right)\end{pmatrix}
\end{aligned}
$$

$$
\begin{aligned}
L_{32} = {} & \frac{-1}{xt}\left(\frac{A_{22}}{xs}\frac{\partial}{\partial\theta}+A_{26}\left(\frac{\partial}{\partial x}-\frac{1}{x}\right)+\frac{B_{22}c}{x^2s^2}\frac{\partial}{\partial\theta}+\frac{B_{26}}{xt}\left(\frac{\partial}{\partial x}-\frac{2}{x}\right)\right) \\
& +\frac{\partial}{\partial x}\begin{pmatrix}\frac{\partial}{\partial x}\left(\frac{B_{12}}{xs}\frac{\partial}{\partial\theta}+B_{16}\left(\frac{\partial}{\partial x}-\frac{1}{x}\right)+\frac{D_{12}c}{x^2s^2}\frac{\partial}{\partial\theta}+\frac{D_{16}}{xt}\left(\frac{\partial}{\partial x}-\frac{2}{x}\right)\right)\\ +\frac{1}{xs}\frac{\partial}{\partial\theta}\left(\frac{B_{26}}{xs}\frac{\partial}{\partial\theta}+B_{66}\left(\frac{\partial}{\partial x}-\frac{1}{x}\right)+\frac{D_{26}c}{x^2s^2}\frac{\partial}{\partial\theta}+\frac{D_{66}}{xt}\left(\frac{\partial}{\partial x}-\frac{2}{x}\right)\right)\\ +\frac{1}{x}\left(\frac{B_{12}}{xs}\frac{\partial}{\partial\theta}+B_{16}\left(\frac{\partial}{\partial x}-\frac{1}{x}\right)+\frac{D_{12}c}{x^2s^2}\frac{\partial}{\partial\theta}+\frac{D_{16}}{xt}\left(\frac{\partial}{\partial x}-\frac{2}{x}\right)\right)\\ -\frac{1}{x}\left(\frac{B_{22}}{xs}\frac{\partial}{\partial\theta}+B_{26}\left(\frac{\partial}{\partial x}-\frac{1}{x}\right)+\frac{D_{22}c}{x^2s^2}\frac{\partial}{\partial\theta}+\frac{D_{26}}{xt}\left(\frac{\partial}{\partial x}-\frac{2}{x}\right)\right)\end{pmatrix} \\
& +\frac{1}{x}\begin{pmatrix}\frac{\partial}{\partial x}\left(\frac{B_{12}}{xs}\frac{\partial}{\partial\theta}+B_{16}\left(\frac{\partial}{\partial x}-\frac{1}{x}\right)+\frac{D_{12}c}{x^2s^2}\frac{\partial}{\partial\theta}+\frac{D_{16}}{xt}\left(\frac{\partial}{\partial x}-\frac{2}{x}\right)\right)\\ +\frac{1}{xs}\frac{\partial}{\partial\theta}\left(\frac{B_{26}}{xs}\frac{\partial}{\partial\theta}+B_{66}\left(\frac{\partial}{\partial x}-\frac{1}{x}\right)+\frac{D_{26}c}{x^2s^2}\frac{\partial}{\partial\theta}+\frac{D_{66}}{xt}\left(\frac{\partial}{\partial x}-\frac{2}{x}\right)\right)\\ +\frac{1}{x}\left(\frac{B_{12}}{xs}\frac{\partial}{\partial\theta}+B_{16}\left(\frac{\partial}{\partial x}-\frac{1}{x}\right)+\frac{D_{12}c}{x^2s^2}\frac{\partial}{\partial\theta}+\frac{D_{16}}{xt}\left(\frac{\partial}{\partial x}-\frac{2}{x}\right)\right)\\ -\frac{1}{x}\left(\frac{B_{22}}{xs}\frac{\partial}{\partial\theta}+B_{26}\left(\frac{\partial}{\partial x}-\frac{1}{x}\right)+\frac{D_{22}c}{x^2s^2}\frac{\partial}{\partial\theta}+\frac{D_{26}}{xt}\left(\frac{\partial}{\partial x}-\frac{2}{x}\right)\right)\end{pmatrix} \\
& +\frac{1}{xs}\frac{\partial}{\partial\theta}\begin{pmatrix}\frac{1}{xs}\frac{\partial}{\partial\theta}\left(\frac{B_{22}}{xs}\frac{\partial}{\partial\theta}+B_{26}\left(\frac{\partial}{\partial x}-\frac{1}{x}\right)+\frac{D_{22}c}{x^2s^2}\frac{\partial}{\partial\theta}+\frac{D_{26}}{xt}\left(\frac{\partial}{\partial x}-\frac{2}{x}\right)\right)\\ +\frac{\partial}{\partial x}\left(\frac{B_{26}}{xs}\frac{\partial}{\partial\theta}+B_{66}\left(\frac{\partial}{\partial x}-\frac{1}{x}\right)+\frac{D_{26}c}{x^2s^2}\frac{\partial}{\partial\theta}+\frac{D_{66}}{xt}\left(\frac{\partial}{\partial x}-\frac{2}{x}\right)\right)\\ +\frac{2}{x}\left(\frac{B_{26}}{xs}\frac{\partial}{\partial\theta}+B_{66}\left(\frac{\partial}{\partial x}-\frac{1}{x}\right)+\frac{D_{26}c}{x^2s^2}\frac{\partial}{\partial\theta}+\frac{D_{66}}{xt}\left(\frac{\partial}{\partial x}-\frac{2}{x}\right)\right)\end{pmatrix}
\end{aligned}
$$

$$
\begin{aligned}
L_{33} = {} & \frac{-1}{xt}\left(\frac{A_{22}}{xt}-B_{12}\frac{\partial^2}{\partial x^2}+\frac{B_{22}}{x}\left(\frac{\partial^2}{xs^2\partial\theta^2}+\frac{\partial}{\partial x}\right)-\frac{B_{26}}{xs}\left(\frac{2\partial^2}{\partial x\partial\theta}-\frac{2\partial}{x\partial\theta}\right)\right) \\
& +\frac{\partial}{\partial x}\begin{pmatrix}\frac{\partial}{\partial x}\left(\frac{B_{12}}{xt}-D_{11}\frac{\partial^2}{\partial x^2}+\frac{D_{12}}{x}\left(\frac{\partial^2}{xs^2\partial\theta^2}+\frac{\partial}{\partial x}\right)-\frac{D_{16}}{xs}\left(\frac{2\partial^2}{\partial x\partial\theta}-\frac{2\partial}{x\partial\theta}\right)\right)\\ +\frac{1}{xs}\frac{\partial}{\partial\theta}\left(\frac{B_{26}}{xt}-D_{16}\frac{\partial^2}{\partial x^2}+\frac{D_{26}}{x}\left(\frac{\partial^2}{xs^2\partial\theta^2}+\frac{\partial}{\partial x}\right)-\frac{D_{66}}{xs}\left(\frac{2\partial^2}{\partial x\partial\theta}-\frac{2\partial}{x\partial\theta}\right)\right)\\ +\frac{1}{x}\left(\frac{B_{12}}{xt}-D_{11}\frac{\partial^2}{\partial x^2}+\frac{D_{12}}{x}\left(\frac{\partial^2}{xs^2\partial\theta^2}+\frac{\partial}{\partial x}\right)-\frac{D_{16}}{xs}\left(\frac{2\partial^2}{\partial x\partial\theta}-\frac{2\partial}{x\partial\theta}\right)\right)\\ -\frac{1}{x}\left(\frac{B_{22}}{xt}-D_{12}\frac{\partial^2}{\partial x^2}+\frac{D_{22}}{x}\left(\frac{\partial^2}{xs^2\partial\theta^2}+\frac{\partial}{\partial x}\right)-\frac{D_{26}}{xs}\left(\frac{2\partial^2}{\partial x\partial\theta}-\frac{2\partial}{x\partial\theta}\right)\right)\end{pmatrix}
\end{aligned}
$$

$$
\begin{aligned}
L_{33} = {} & \frac{-1}{xt}\left(\frac{A_{22}}{xt} - B_{12}\frac{\partial^2}{\partial x^2} + \frac{B_{22}}{x}\left(\frac{\partial^2}{xs^2\partial\theta^2} + \frac{\partial}{\partial x}\right) - \frac{B_{26}}{xs}\left(\frac{2\partial^2}{\partial x\partial\theta} - \frac{2\partial}{x\partial\theta}\right)\right) \\
& + \frac{\partial}{\partial x}\begin{pmatrix}
\frac{\partial}{\partial x}\left(\frac{B_{12}}{xt} - D_{11}\frac{\partial^2}{\partial x^2} + \frac{D_{12}}{x}\left(\frac{\partial^2}{xs^2\partial\theta^2} + \frac{\partial}{\partial x}\right) - \frac{D_{16}}{xs}\left(\frac{2\partial^2}{\partial x\partial\theta} - \frac{2\partial}{x\partial\theta}\right)\right) \\
+\frac{1}{xs}\frac{\partial}{\partial\theta}\left(\frac{B_{26}}{xt} - D_{16}\frac{\partial^2}{\partial x^2} + \frac{D_{26}}{x}\left(\frac{\partial^2}{xs^2\partial\theta^2} + \frac{\partial}{\partial x}\right) - \frac{D_{66}}{xs}\left(\frac{2\partial^2}{\partial x\partial\theta} - \frac{2\partial}{x\partial\theta}\right)\right) \\
+\frac{1}{x}\left(\frac{B_{12}}{xt} - D_{11}\frac{\partial^2}{\partial x^2} + \frac{D_{12}}{x}\left(\frac{\partial^2}{xs^2\partial\theta^2} + \frac{\partial}{\partial x}\right) - \frac{D_{16}}{xs}\left(\frac{2\partial^2}{\partial x\partial\theta} - \frac{2\partial}{x\partial\theta}\right)\right) \\
-\frac{1}{x}\left(\frac{B_{22}}{xt} - D_{12}\frac{\partial^2}{\partial x^2} + \frac{D_{22}}{x}\left(\frac{\partial^2}{xs^2\partial\theta^2} + \frac{\partial}{\partial x}\right) - \frac{D_{26}}{xs}\left(\frac{2\partial^2}{\partial x\partial\theta} - \frac{2\partial}{x\partial\theta}\right)\right)
\end{pmatrix} \\
& + \frac{1}{x}\begin{pmatrix}
\frac{\partial}{\partial x}\left(\frac{B_{12}}{xt} - D_{11}\frac{\partial^2}{\partial x^2} + \frac{D_{12}}{x}\left(\frac{\partial^2}{xs^2\partial\theta^2} + \frac{\partial}{\partial x}\right) - \frac{D_{16}}{xs}\left(\frac{2\partial^2}{\partial x\partial\theta} - \frac{2\partial}{x\partial\theta}\right)\right) \\
+\frac{1}{xs}\frac{\partial}{\partial\theta}\left(\frac{B_{26}}{xt} - D_{16}\frac{\partial^2}{\partial x^2} + \frac{D_{26}}{x}\left(\frac{\partial^2}{xs^2\partial\theta^2} + \frac{\partial}{\partial x}\right) - \frac{D_{66}}{xs}\left(\frac{2\partial^2}{\partial x\partial\theta} - \frac{2\partial}{x\partial\theta}\right)\right) \\
+\frac{1}{x}\left(\frac{B_{12}}{xt} - D_{11}\frac{\partial^2}{\partial x^2} + \frac{D_{12}}{x}\left(\frac{\partial^2}{xs^2\partial\theta^2} + \frac{\partial}{\partial x}\right) - \frac{D_{16}}{xs}\left(\frac{2\partial^2}{\partial x\partial\theta} - \frac{2\partial}{x\partial\theta}\right)\right) \\
-\frac{1}{x}\left(\frac{B_{22}}{xt} - D_{12}\frac{\partial^2}{\partial x^2} + \frac{D_{22}}{x}\left(\frac{\partial^2}{xs^2\partial\theta^2} + \frac{\partial}{\partial x}\right) - \frac{D_{26}}{xs}\left(\frac{2\partial^2}{\partial x\partial\theta} - \frac{2\partial}{x\partial\theta}\right)\right)
\end{pmatrix} \\
& + \frac{1}{xs}\frac{\partial}{\partial\theta}\begin{pmatrix}
\frac{1}{xs}\frac{\partial}{\partial\theta}\left(\frac{B_{22}}{xt} - D_{12}\frac{\partial^2}{\partial x^2} + \frac{D_{22}}{x}\left(\frac{\partial^2}{xs^2\partial\theta^2} + \frac{\partial}{\partial x}\right) - \frac{D_{26}}{xs}\left(\frac{2\partial^2}{\partial x\partial\theta} - \frac{2\partial}{x\partial\theta}\right)\right) \\
+\frac{\partial}{\partial x}\left(\frac{B_{26}}{xt} - D_{16}\frac{\partial^2}{\partial x^2} + \frac{D_{26}}{x}\left(\frac{\partial^2}{xs^2\partial\theta^2} + \frac{\partial}{\partial x}\right) - \frac{D_{66}}{xs}\left(\frac{2\partial^2}{\partial x\partial\theta} - \frac{2\partial}{x\partial\theta}\right)\right) \\
+\frac{2}{x}\left(\frac{B_{26}}{xt} - D_{16}\frac{\partial^2}{\partial x^2} + \frac{D_{26}}{x}\left(\frac{\partial^2}{xs^2\partial\theta^2} + \frac{\partial}{\partial x}\right) - \frac{D_{66}}{xs}\left(\frac{2\partial^2}{\partial x\partial\theta} - \frac{2\partial}{x\partial\theta}\right)\right)
\end{pmatrix}
\end{aligned} \tag{6.13}
$$

The above equations show the level of complexity in solving the governing equations of a general laminated conical shell. When a conical shell is laminated symmetrically with respect to its middle surface, the constants B_{ij} equal to zero, and, hence the equations are much simplified. Substituting Eq. (6.2) into Eqs. (1.29) and (1.30), the general boundary conditions of thin conical shells are:

$$
\begin{aligned}
R = R_0{:}&\begin{cases}
N_x - k^u_{x0}u = 0 \\
N_{x\theta} + \frac{cM_{x\theta}}{R_0} - k^v_{x0}v = 0 \\
Q_x + \frac{\partial M_{x\theta}}{R_0\partial\theta} - k^w_{x0}w = 0 \\
-M_x - K^w_{x0}\frac{\partial w}{\partial x} = 0
\end{cases}
\qquad
R = R_1{:}\begin{cases}
N_x + k^u_{x1}u = 0 \\
N_{x\theta} + \frac{cM_{x\theta}}{R_1} + k^v_{x1}v = 0 \\
Q_x + \frac{\partial M_{x\theta}}{R_1\partial\theta} + k^w_{x1}w = 0 \\
-M_x + K^w_{x1}\frac{\partial w}{\partial x} = 0
\end{cases} \\
\theta = 0{:}&\begin{cases}
N_{x\theta} - k^u_{\theta 0}u = 0 \\
N_\theta + \frac{cM_\theta}{R_0} - k^v_{\theta 0}v = 0 \\
Q_\theta + \frac{\partial M_{x\theta}}{\partial x} - k^w_{\theta 0}w = 0 \\
-M_\theta - K^w_{\theta 0}\frac{\partial w}{R_0\partial\theta} = 0
\end{cases}
\qquad
\theta = \theta_0{:}\begin{cases}
N_{x\theta} + k^u_{\theta 1}u = 0 \\
N_\theta + \frac{cM_\theta}{R_1} + k^v_{\theta 1}v = 0 \\
Q_\theta + \frac{\partial M_{x\theta}}{\partial x} + k^w_{\theta 1}w = 0 \\
-M_\theta + K^w_{\theta 1}\frac{\partial w}{R_1\partial\theta} = 0
\end{cases}
\end{aligned} \tag{6.14}
$$

Alternately, the governing equations and boundary conditions of thin laminated conical shells can be obtained by the Hamilton's principle in the same manner as described in Sect. 1.2.4.

Table 6.1 Possible classical boundary conditions for thin laminated conical shells at boundary $R = R_0$

Boundary type	Conditions
Free boundary conditions	
F	$N_x = N_{x\theta} + \frac{cM_{x\theta}}{R_0} = Q_x + \frac{\partial M_{x\theta}}{R_0 \partial\theta} = M_x = 0$
F2	$u = N_{x\theta} + \frac{cM_{x\theta}}{R_0} = Q_x + \frac{\partial M_{x\theta}}{R_0 \partial\theta} = M_x = 0$
F3	$N_x = v = Q_x + \frac{\partial M_{x\theta}}{R_0 \partial\theta} = M_x = 0$
F4	$u = v = Q_x + \frac{\partial M_{x\theta}}{R_0 \partial\theta} = M_x = 0$
Simply supported boundary conditions	
S	$u = v = w = M_x = 0$
SD	$N_x = v = w = M_x = 0$
S3	$u = N_{x\theta} + \frac{cM_{x\theta}}{R_0} = w = M_x = 0$
S4	$N_x = N_{x\theta} + \frac{cM_{x\theta}}{R_0} = w = M_x = 0$
Clamped boundary conditions	
C	$u = v = w = \frac{\partial w}{\partial x} = 0$
C2	$N_x = v = w = \frac{\partial w}{\partial x} = 0$
C3	$u = N_{x\theta} + \frac{cM_{x\theta}}{R_0} = w = \frac{\partial w}{\partial x} = 0$
C4	$N_x = N_{x\theta} + \frac{cM_{x\theta}}{R_0} = w = \frac{\partial w}{\partial x} = 0$

Thin conical shells can have up to 12 possible classical boundary conditions at each edge. This yields a numerous combinations of boundary conditions, particular for open conical shells. The possible combinations for each classical boundary conditions at boundary $R = R_0$ are given in Table 6.1. Similar boundary conditions can be obtained for the other three boundaries (i.e., $R = R_1$, $\theta = 0$ and $\theta = \theta_0$).

6.2 Fundamental Equations of Thick Laminated Conical Shells

The fundamental equations of thin laminated conical shells presented in the previous section are based on the CST and are applicable only when the total thickness of a shell is smaller than 1/20 of the smallest of the wave lengths and/or radii of curvature (Qatu 2004) due to the fact that both shear deformation and rotary inertia are neglected in the formulation. Fundamental equations of thick laminated conical shells will be derived in this section. As usual, the equations that follow are a specialization of the general first-order shear deformation shell theory (see Sect. 1.3) to those of thick laminated conical shells.

6.2.1 Kinematic Relations

On the basis of the assumptions of the SDST, the displacement field of a conical shell is expressed in terms of the middle surface displacements and rotation components as

$$\begin{aligned} U(x,\theta,z) &= u(x,\theta) + z\phi_x \\ V(x,\theta,z) &= v(x,\theta) + z\phi_\theta \\ W(x,\theta,z) &= w(x,\theta) \end{aligned} \tag{6.15}$$

where u, v and w are the middle surface displacements of the shell in the x, θ and z directions, respectively, and ϕ_x and ϕ_θ represent the rotations of the transverse normal respect to θ- and x-axes.

Specializing Eqs. (1.33) and (1.34) to those of conical shells, the normal and shear strains at any point of the shell space can be defined as:

$$\begin{aligned} \varepsilon_x &= \varepsilon_x^0 + z\chi_x \\ \varepsilon_\theta &= \frac{1}{(1+z/R_\theta)}\left(\varepsilon_\theta^0 + z\chi_\theta\right) \\ \gamma_{x\theta} &= \left(\gamma_{x\theta}^0 + z\chi_{x\theta}\right) + \frac{1}{(1+z/R_\theta)}\left(\gamma_{\theta x}^0 + z\chi_{\theta x}\right) \\ \gamma_{xz} &= \gamma_{xz}^0 \\ \gamma_{\theta z} &= \frac{\gamma_{\theta z}^0}{(1+z/R_\theta)} \end{aligned} \tag{6.16}$$

where ε_x^0, ε_θ^0, $\gamma_{x\theta}^0$ and $\gamma_{\theta x}^0$ are the normal and shear strains. χ_x, χ_θ, $\chi_{x\theta}$ and $\chi_{\theta x}$ denote the curvature and twist changes; γ_{xz}^0 and $\gamma_{\theta z}^0$ represent the transverse shear strains. They are defined in terms of the middle surface displacements and rotation components as:

$$\begin{aligned} \varepsilon_x^0 &= \frac{\partial u}{\partial x} & \chi_x &= \frac{\partial \phi_x}{\partial x} \\ \varepsilon_\theta^0 &= \frac{\partial v}{xs\partial\theta} + \frac{u}{x} + \frac{w}{xt} & \chi_\theta &= \frac{\partial \phi_\theta}{xs\partial\theta} + \frac{\phi_x}{x} \\ \gamma_{x\theta}^0 &= \frac{\partial v}{\partial x} & \chi_{x\theta} &= \frac{\partial \phi_\theta}{\partial x} \\ \gamma_{\theta x}^0 &= \frac{\partial u}{xs\partial\theta} - \frac{v}{x} & \chi_{x\theta} &= \frac{\partial \phi_x}{xs\partial\theta} - \frac{\phi_\theta}{x} \\ \gamma_{xz}^0 &= \frac{\partial w}{\partial x} + \phi_x & \gamma_{\theta z}^0 &= \frac{\partial w}{xs\partial\theta} - \frac{v}{xt} + \phi_\theta \end{aligned} \tag{6.17}$$

6.2.2 Stress-Strain Relations and Stress Resultants

The stress-strain relations derived earlier for the thick cylindrical shells [i.e., Eq. (5.20)] are applicable for the conical shells. Substituting Eq. (6.2) into (1.40), the force and moment resultants of a thick conical shell can be obtained by following integration operation:

$$\begin{bmatrix} N_x \\ N_{x\theta} \\ Q_x \end{bmatrix} = \int_{-h/2}^{h/2} \begin{bmatrix} \sigma_x \\ \tau_{x\theta} \\ \tau_{xz} \end{bmatrix} \left(1 + \tfrac{z}{R_\theta}\right) dz \quad \begin{bmatrix} N_\theta \\ N_{\theta x} \\ Q_\theta \end{bmatrix} = \int_{-h/2}^{h/2} \begin{bmatrix} \sigma_\theta \\ \tau_{\theta x} \\ \tau_{\theta z} \end{bmatrix} dz$$
$$\begin{bmatrix} M_x \\ M_{x\theta} \end{bmatrix} = \int_{-h/2}^{h/2} \begin{bmatrix} \sigma_x \\ \tau_{x\theta} \end{bmatrix} \left(1 + \tfrac{z}{R_\theta}\right) z dz \quad \begin{bmatrix} M_\theta \\ M_{\theta x} \end{bmatrix} = \int_{-h/2}^{h/2} \begin{bmatrix} \sigma_\theta \\ \tau_{\theta x} \end{bmatrix} z dz \tag{6.18}$$

Since the radius of curvature R_θ is a function of the x coordinate, thus, the resulting stiffness parameters will be functions of the x coordinate. This will results in much complexity in equations of thick conical shells. Qatu (2004) suggested taking the average curvature of the conical shells when using these equations. Figures 3.7 and 3.8 showed that the effects of the deepness term z/R on the frequency parameters of an extremely deep, unsymmetrically laminated curved beam ($\theta_0 = 286.48°$) with thickness-to-radius ratio $h/R = 0.1$ is very small and the maximum effect is less than 0.41 % for the worse case. It is proposed here to neglect the effects of the deepness term z/R_β. In many prior researches, the effects of the deepness term z/R_β are often neglected (for example, Jin et al. 2013b, 2014a; Qu et al. 2013a, b; Ye et al. 2014b). Neglecting the effects of the deepness term, the force and moment resultants of a thick conical shell can be rewritten as:

$$\begin{bmatrix} N_x \\ N_\theta \\ N_{x\theta} \\ N_{\theta x} \\ M_x \\ M_\theta \\ M_{x\theta} \\ M_{\theta x} \end{bmatrix} = \begin{bmatrix} A_{11} & A_{12} & A_{16} & A_{16} & B_{11} & B_{12} & B_{16} & B_{16} \\ A_{12} & A_{22} & A_{26} & A_{26} & B_{12} & B_{22} & B_{26} & B_{26} \\ A_{16} & A_{26} & A_{66} & A_{66} & B_{16} & B_{26} & B_{66} & B_{66} \\ A_{16} & A_{26} & A_{66} & A_{66} & B_{16} & B_{26} & B_{66} & B_{66} \\ B_{11} & B_{12} & B_{16} & B_{16} & D_{11} & D_{12} & D_{16} & D_{16} \\ B_{12} & B_{22} & B_{26} & B_{26} & D_{12} & D_{22} & D_{26} & D_{26} \\ B_{16} & B_{26} & B_{66} & B_{66} & D_{16} & D_{26} & D_{66} & D_{66} \\ B_{16} & B_{26} & B_{66} & B_{66} & D_{16} & D_{26} & D_{66} & D_{66} \end{bmatrix} \begin{bmatrix} \varepsilon_x^0 \\ \varepsilon_\theta^0 \\ \gamma_{x\theta}^0 \\ \gamma_{\theta x}^0 \\ \chi_x \\ \chi_\theta \\ \chi_{x\theta} \\ \chi_{\theta x} \end{bmatrix} \tag{6.19a}$$

$$\begin{bmatrix} Q_\theta \\ Q_x \end{bmatrix} = \begin{bmatrix} A_{44} & A_{45} \\ A_{45} & A_{55} \end{bmatrix} \begin{bmatrix} \gamma_{\theta z}^0 \\ \gamma_{xz}^0 \end{bmatrix} \tag{6.19b}$$

The stiffness coefficients A_{ij}, B_{ij} and D_{ij} are given as in Eq. (1.43).

6.2.3 Energy Functions

The strain energy (U_s) of thick conical shells during vibration can be defined in terms of the middle surface strains and curvature changes and stress resultants as

$$U_s = \frac{1}{2}\int_x \int_\theta \left\{ \begin{array}{l} N_x\varepsilon_x^0 + N_\theta\varepsilon_\theta^0 + N_{x\theta}\gamma_{x\theta}^0 + N_{\theta x}\gamma_{\theta x}^0 + M_x\chi_x \\ +M_\theta\chi_\theta + M_{x\theta}\chi_{x\theta} + M_{\theta x}\chi_{\theta x} + Q_\theta\gamma_{\theta z} + Q_x\gamma_{xz} \end{array} \right\} xsd\theta dx \tag{6.20}$$

Substituting Eqs. (6.17) and (6.19a, 6.19b) into Eq. (6.20), the strain energy of the shell can be expressed in terms of the middle surface displacements (u, v, w) and rotation components (ϕ_x, ϕ_θ) as:

$$\begin{aligned} U_s = {} & \frac{1}{2}\int_x \int_\theta \left\{ \begin{array}{l} A_{11}\left(\frac{\partial u}{\partial x}\right)^2 + 2A_{12}\left(\frac{\partial v}{xs\partial\theta} + \frac{u}{x} + \frac{w}{xt}\right)\left(\frac{\partial u}{\partial x}\right) \\ +2A_{16}\left(\frac{\partial v}{\partial x} + \frac{\partial u}{xs\partial\theta} - \frac{v}{x}\right)\left(\frac{\partial u}{\partial x}\right) + A_{22}\left(\frac{\partial v}{xs\partial\theta} + \frac{u}{x} + \frac{w}{xt}\right)^2 \\ +2A_{26}\left(\frac{\partial v}{\partial x} + \frac{\partial u}{xs\partial\theta} - \frac{v}{x}\right)\left(\frac{\partial v}{xs\partial\theta} + \frac{u}{x} + \frac{w}{xt}\right) \\ +A_{66}\left(\frac{\partial v}{\partial x} + \frac{\partial u}{xs\partial\theta} - \frac{v}{x}\right)^2 + A_{44}\left(\frac{\partial w}{xs\partial\theta} - \frac{v}{xt} + \phi_\theta\right)^2 \\ +2A_{45}\left(\frac{\partial w}{xs\partial\theta} - \frac{v}{xt} + \phi_\theta\right)\left(\frac{\partial w}{\partial x} + \phi_x\right) + A_{55}\left(\frac{\partial w}{\partial x} + \phi_x\right)^2 \end{array} \right\} xsd\theta dx \\ & + \int_x \int_\theta \left\{ \begin{array}{l} B_{11}\left(\frac{\partial\phi_x}{\partial x}\right)\left(\frac{\partial u}{\partial x}\right) + B_{12}\left(\frac{\partial\phi_\theta}{xs\partial\theta} + \frac{\phi_x}{x}\right)\left(\frac{\partial u}{\partial x}\right) \\ +B_{16}\left(\frac{\partial\phi_\theta}{\partial x} + \frac{\partial\phi_x}{xs\partial\theta} - \frac{\phi_\theta}{x}\right)\left(\frac{\partial u}{\partial x}\right) + B_{12}\left(\frac{\partial\phi_x}{\partial x}\right) \\ \times\left(\frac{\partial v}{xs\partial\theta} + \frac{u}{x} + \frac{w}{xt}\right) + B_{22}\left(\frac{\partial\phi_\theta}{xs\partial\theta} + \frac{\phi_x}{x}\right) \\ \times\left(\frac{\partial v}{xs\partial\theta} + \frac{u}{x} + \frac{w}{xt}\right) + B_{26}\left(\frac{\partial\phi_\theta}{\partial x} + \frac{\partial\phi_x}{xs\partial\theta} - \frac{\phi_\theta}{x}\right) \\ \times\left(\frac{\partial v}{xs\partial\theta} + \frac{u}{x} + \frac{w}{xt}\right) + B_{16}\left(\frac{\partial\phi_x}{\partial x}\right)\left(\frac{\partial v}{\partial x} + \frac{\partial u}{xs\partial\theta} - \frac{v}{x}\right) \\ +B_{26}\left(\frac{\partial\phi_\theta}{xs\partial\theta} + \frac{\phi_x}{x}\right)\left(\frac{\partial v}{\partial x} + \frac{\partial u}{xs\partial\theta} - \frac{v}{x}\right) \\ +B_{66}\left(\frac{\partial\phi_\theta}{\partial x} + \frac{\partial\phi_x}{xs\partial\theta} - \frac{\phi_\theta}{x}\right)\left(\frac{\partial v}{\partial x} + \frac{\partial u}{xs\partial\theta} - \frac{v}{x}\right) \end{array} \right\} xsd\theta dx \\ & + \frac{1}{2}\int_x \int_\theta \left\{ \begin{array}{l} D_{11}\left(\frac{\partial\phi_x}{\partial x}\right)^2 + 2D_{12}\left(\frac{\partial\phi_\theta}{xs\partial\theta} + \frac{\phi_x}{x}\right)\left(\frac{\partial\phi_x}{\partial x}\right) \\ +2D_{16}\left(\frac{\partial\phi_\theta}{\partial x} + \frac{\partial\phi_x}{xs\partial\theta} - \frac{\phi_\theta}{x}\right)\left(\frac{\partial\phi_x}{\partial x}\right) \\ +D_{22}\left(\frac{\partial\phi_\theta}{xs\partial\theta} + \frac{\phi_x}{x}\right)^2 + 2D_{26}\left(\frac{\partial\phi_\theta}{\partial x} + \frac{\partial\phi_x}{xs\partial\theta} - \frac{\phi_\theta}{x}\right) \\ \times\left(\frac{\partial\phi_\theta}{xs\partial\theta} + \frac{\phi_x}{x}\right) + D_{66}\left(\frac{\partial\phi_\theta}{\partial x} + \frac{\partial\phi_x}{xs\partial\theta} - \frac{\phi_\theta}{x}\right)^2 \end{array} \right\} xsd\theta dx \end{aligned} \tag{6.21}$$

and the kinetic energy (T) function can be written as:

$$T = \frac{1}{2}\int_x \int_\theta \left\{ \begin{array}{l} I_0\left(\frac{\partial u}{\partial t}\right)^2 + 2I_1 \frac{\partial u}{\partial t}\frac{\partial \phi_x}{\partial t} + I_2\left(\frac{\partial \phi_x}{\partial t}\right)^2 + I_0\left(\frac{\partial v}{\partial t}\right)^2 \\ +2I_1 \frac{\partial v}{\partial t}\frac{\partial \phi_\theta}{\partial t} + I_2\left(\frac{\partial \phi_\theta}{\partial t}\right)^2 + I_0\left(\frac{\partial w}{\partial t}\right)^2 \end{array} \right\} xsd\theta dx \tag{6.22}$$

where the inertia terms are given as in Eq. (1.52).

Suppose the shell is subjected to external forces q_x, q_θ and q_z (in the x, θ and z directions, respectively) and external couples m_x and m_θ (in the middle surface), thus, the work done by the external forces and moments is written as

$$W_e = \int_x \int_\theta \{q_x u + q_\theta v + q_z w + m_x \phi_x + m_\theta \phi_\theta\} xsd\theta dx \tag{6.23}$$

Using the artificial spring boundary technique similar to that described earlier, let k_ψ^u, k_ψ^v, k_ψ^w, K_ψ^x and $K_\psi^\theta (\psi = x_0, \theta_0, x_1$ and $\theta_1)$ to represent the rigidities (per unit length) of the boundary springs at the boundaries $R = R_0$, $\theta = 0$, $R = R_1$ and $\theta = \theta_0$, respectively. Therefore, the deformation strain energy (U_{sp}) of the boundary springs during vibration is:

$$\begin{aligned} U_{sp} = & \frac{1}{2}\int_\theta \left\{ \begin{array}{l} x\left[k_{x0}^u u^2 + k_{x0}^v v^2 + k_{x0}^w w^2 + K_{x0}^x \phi_x^2 + K_{x0}^\theta \phi_\theta^2\right]|_{R=R_0} \\ +x\left[k_{x1}^u u^2 + k_{x1}^v v^2 + k_{x1}^w w^2 + K_{x1}^x \phi_x^2 + K_{x1}^\theta \phi_\theta^2\right]|_{R=R_1} \end{array} \right\} xsd\theta \\ & + \frac{1}{2}\int_x \left\{ \begin{array}{l} \left[k_{\theta 0}^u u^2 + k_{\theta 0}^v v^2 + k_{\theta 0}^w w^2 + K_{\theta 0}^x \phi_x^2 + K_{\theta 0}^\theta \phi_\theta^2\right]|_{\theta=0} \\ +\left[k_{\theta 1}^u u^2 + k_{\theta 1}^v v^2 + k_{\theta 1}^w w^2 + K_{\theta 1}^x \phi_x^2 + K_{\theta 1}^\theta \phi_\theta^2\right]|_{\theta=\theta_0} \end{array} \right\} dx \end{aligned} \tag{6.24}$$

6.2.4 Governing Equations and Boundary Conditions

The governing equations and boundary conditions of thick laminated conical shells can be obtained by the Hamilton's principle in the same manner as described in Sect. 1.2.4. Alternately, it can be specialized from those of general thick shells by substituting Eq. (6.2) into Eq. (1.59). According to Eq. (1.59), we have (after being divided by $B = xs$)

$$
\begin{aligned}
&\frac{\partial N_x}{\partial x}+\frac{N_x-N_\theta}{x}+\frac{\partial N_{\theta x}}{xs\partial\theta}+q_x=I_0\frac{\partial^2 u}{\partial t^2}+I_1\frac{\partial^2\phi_x}{\partial t^2}\\
&\frac{\partial N_{x\theta}}{\partial x}+\frac{\partial N_\theta}{xs\partial\theta}+\frac{N_{x\theta}+N_{\theta x}}{x}+\frac{Q_\theta}{xt}+q_\theta=I_0\frac{\partial^2 v}{\partial t^2}+I_1\frac{\partial^2\phi_\theta}{\partial t^2}\\
&-\frac{N_\theta}{xt}+\frac{\partial Q_x}{\partial x}+\frac{Q_x}{x}+\frac{\partial Q_\theta}{xs\partial\theta}+q_z=I_0\frac{\partial^2 w}{\partial t^2}\\
&\frac{\partial M_x}{\partial x}+\frac{M_x-M_\theta}{x}+\frac{\partial M_{\theta x}}{xs\partial\theta}-Q_x+m_x=I_1\frac{\partial^2 u}{\partial t^2}+I_2\frac{\partial^2\phi_x}{\partial t^2}\\
&\frac{\partial M_{x\theta}}{\partial x}+\frac{\partial M_\theta}{xs\partial\theta}+\frac{M_{x\theta}+M_{\theta x}}{x}-Q_\theta+m_\theta=I_1\frac{\partial^2 v}{\partial t^2}+I_2\frac{\partial^2\phi_\theta}{\partial t^2}
\end{aligned}
\tag{6.25}
$$

Substituting Eqs. (6.17) and (6.19a, 6.19b) into above equation, the governing equations can be written in terms of displacements as

$$
\left(\begin{bmatrix}L_{11}&L_{12}&L_{13}&L_{14}&L_{15}\\L_{21}&L_{22}&L_{23}&L_{24}&L_{25}\\L_{31}&L_{32}&L_{33}&L_{34}&L_{35}\\L_{41}&L_{42}&L_{43}&L_{44}&L_{45}\\L_{51}&L_{52}&L_{53}&L_{54}&L_{55}\end{bmatrix}+\omega^2\begin{bmatrix}I_0&0&0&I_1&0\\0&I_0&0&0&I_1\\0&0&I_0&0&0\\I_1&0&0&I_2&0\\0&I_1&0&0&I_2\end{bmatrix}\right)\begin{bmatrix}u\\v\\w\\\phi_x\\\phi_\theta\end{bmatrix}=\begin{bmatrix}-p_x\\-p_y\\-p_z\\-m_x\\-m_\theta\end{bmatrix}
\tag{6.26}
$$

The coefficients of the linear operator L_{ij} are given as

$$
\begin{aligned}
L_{11}=&\frac{\partial}{\partial x}\left(A_{11}\frac{\partial}{\partial x}+\frac{A_{12}}{x}+\frac{A_{16}}{xs}\frac{\partial}{\partial\theta}\right)+\frac{1}{x}\left(A_{11}\frac{\partial}{\partial x}+\frac{A_{12}}{x}+\frac{A_{16}}{xs}\frac{\partial}{\partial\theta}\right)\\
&-\frac{1}{x}\left(A_{12}\frac{\partial}{\partial x}+\frac{A_{22}}{x}+\frac{A_{26}}{xs}\frac{\partial}{\partial\theta}\right)+\frac{1}{xs}\frac{\partial}{\partial\theta}\left(A_{16}\frac{\partial}{\partial x}+\frac{A_{26}}{x}+\frac{A_{66}}{xs}\frac{\partial}{\partial\theta}\right)\\
L_{12}=&\frac{\partial}{\partial x}\left(\frac{A_{12}}{xs}\frac{\partial}{\partial\theta}+A_{16}\left(\frac{\partial}{\partial x}-\frac{1}{x}\right)\right)+\frac{1}{x}\left(\frac{A_{12}}{xs}\frac{\partial}{\partial\theta}+A_{16}\left(\frac{\partial}{\partial x}-\frac{1}{x}\right)\right)\\
&-\frac{1}{x}\left(\frac{A_{22}}{xs}\frac{\partial}{\partial\theta}+A_{26}\left(\frac{\partial}{\partial x}-\frac{1}{x}\right)\right)+\frac{1}{xs}\frac{\partial}{\partial\theta}\left(\frac{A_{26}}{xs}\frac{\partial}{\partial\theta}+A_{66}\left(\frac{\partial}{\partial x}-\frac{1}{x}\right)\right)\\
L_{13}=&\frac{\partial}{\partial x}\left(\frac{A_{12}}{xt}\right)+\frac{1}{x}\left(\frac{A_{12}}{xt}\right)-\frac{1}{x}\left(\frac{A_{22}}{xt}\right)+\frac{1}{xs}\frac{\partial}{\partial\theta}\left(\frac{A_{26}}{xt}\right)\\
L_{14}=&\frac{\partial}{\partial x}\left(B_{11}\frac{\partial}{\partial x}+\frac{B_{12}}{x}+\frac{B_{16}}{xs}\frac{\partial}{\partial\theta}\right)+\frac{1}{x}\left(B_{11}\frac{\partial}{\partial x}+\frac{B_{12}}{x}+\frac{B_{16}}{xs}\frac{\partial}{\partial\theta}\right)\\
&-\frac{1}{x}\left(B_{12}\frac{\partial}{\partial x}+\frac{B_{22}}{x}+\frac{B_{26}}{xs}\frac{\partial}{\partial\theta}\right)+\frac{1}{xs}\frac{\partial}{\partial\theta}\left(B_{16}\frac{\partial}{\partial x}+\frac{B_{26}}{x}+\frac{B_{66}}{xs}\frac{\partial}{\partial\theta}\right)\\
L_{15}=&\frac{\partial}{\partial x}\left(\frac{B_{12}}{xs}\frac{\partial}{\partial\theta}+B_{16}\left(\frac{\partial}{\partial x}-\frac{1}{x}\right)\right)+\frac{1}{x}\left(\frac{B_{12}}{xs}\frac{\partial}{\partial\theta}+B_{16}\left(\frac{\partial}{\partial x}-\frac{1}{x}\right)\right)\\
&-\frac{1}{x}\left(\frac{B_{22}}{xs}\frac{\partial}{\partial\theta}+B_{26}\left(\frac{\partial}{\partial x}-\frac{1}{x}\right)\right)+\frac{1}{xs}\frac{\partial}{\partial\theta}\left(\frac{B_{22}}{xs}\frac{\partial}{\partial\theta}+B_{26}\left(\frac{\partial}{\partial x}-\frac{1}{x}\right)\right)\\
L_{21}=&\frac{1}{xs}\frac{\partial}{\partial\theta}\left(A_{12}\frac{\partial}{\partial x}+\frac{A_{22}}{x}+\frac{A_{26}}{xs}\frac{\partial}{\partial\theta}\right)+\frac{\partial}{\partial x}\left(A_{16}\frac{\partial}{\partial x}+\frac{A_{26}}{x}+\frac{A_{66}}{xs}\frac{\partial}{\partial\theta}\right)\\
&+\frac{2}{x}\left(A_{16}\frac{\partial}{\partial x}+\frac{A_{26}}{x}+\frac{A_{66}}{xs}\frac{\partial}{\partial\theta}\right)
\end{aligned}
$$

$$L_{22} = \frac{1}{xs}\frac{\partial}{\partial\theta}\left(\frac{A_{22}}{xs}\frac{\partial}{\partial\theta} + A_{26}\left(\frac{\partial}{\partial x} - \frac{1}{x}\right)\right) + \frac{\partial}{\partial x}\left(\frac{A_{26}}{xs}\frac{\partial}{\partial\theta} + A_{66}\left(\frac{\partial}{\partial x} - \frac{1}{x}\right)\right) + \frac{2}{x}\left(\frac{A_{26}}{xs}\frac{\partial}{\partial\theta} + A_{66}\left(\frac{\partial}{\partial x} - \frac{1}{x}\right)\right) - \frac{A_{44}}{x^2t^2}$$

$$L_{23} = \frac{1}{xs}\frac{\partial}{\partial\theta}\left(\frac{A_{22}}{xt}\right) + \frac{\partial}{\partial x}\left(\frac{A_{26}}{xt}\right) + \frac{2A_{26}}{x^2t} + \frac{A_{44}}{x^2st}\frac{\partial}{\partial\theta} + \frac{A_{45}}{xt}\frac{\partial}{\partial x}$$

$$L_{24} = \frac{1}{xs}\frac{\partial}{\partial\theta}\left(B_{12}\frac{\partial}{\partial x} + \frac{B_{22}}{x} + \frac{B_{26}}{xs}\frac{\partial}{\partial\theta}\right) + \frac{\partial}{\partial x}\left(B_{16}\frac{\partial}{\partial x} + \frac{B_{26}}{x} + \frac{B_{66}}{xs}\frac{\partial}{\partial\theta}\right) + \frac{2}{x}\left(B_{16}\frac{\partial}{\partial x} + \frac{B_{26}}{x} + \frac{B_{66}}{xs}\frac{\partial}{\partial\theta}\right) + \frac{A_{45}}{xt}$$

$$L_{25} = \frac{1}{xs}\frac{\partial}{\partial\theta}\left(\frac{B_{22}}{xs}\frac{\partial}{\partial\theta} + B_{26}\left(\frac{\partial}{\partial x} - \frac{1}{x}\right)\right) + \frac{\partial}{\partial x}\left(\frac{B_{26}}{xs}\frac{\partial}{\partial\theta} + B_{66}\left(\frac{\partial}{\partial x} - \frac{1}{x}\right)\right) + \frac{2}{x}\left(\frac{B_{26}}{xs}\frac{\partial}{\partial\theta} + B_{66}\left(\frac{\partial}{\partial x} - \frac{1}{x}\right)\right) + \frac{A_{44}}{xt}$$

$$L_{31} = -\frac{A_{12}}{xt}\frac{\partial}{\partial x} - \frac{A_{22}}{x^2t} - \frac{cA_{26}}{x^2s^2}\frac{\partial}{\partial\theta}$$

$$L_{32} = \frac{-1}{xt}\left(\frac{A_{22}}{xs}\frac{\partial}{\partial\theta} + A_{26}\left(\frac{\partial}{\partial x} - \frac{1}{x}\right)\right) - \frac{\partial}{\partial x}\left(\frac{A_{45}}{xt}\right) - \frac{A_{45}}{x^2t} - \frac{cA_{44}}{x^2s^2}\frac{\partial}{\partial\theta}$$

$$L_{33} = \frac{-A_{22}}{x^2t^2} + \frac{\partial}{\partial x}\left(\frac{A_{45}}{xs}\frac{\partial}{\partial\theta} + A_{55}\frac{\partial}{\partial x}\right) + \frac{1}{x}\left(\frac{A_{45}}{xs}\frac{\partial}{\partial\theta} + A_{55}\frac{\partial}{\partial x}\right) + \frac{1}{xs}\frac{\partial}{\partial\theta}\left(\frac{A_{44}}{xs}\frac{\partial}{\partial\theta} + A_{45}\frac{\partial}{\partial x}\right)$$

$$L_{34} = \frac{-1}{xt}\left(B_{12}\frac{\partial}{\partial x} + \frac{B_{22}}{x} + \frac{B_{26}}{xs}\frac{\partial}{\partial\theta}\right) + A_{55}\frac{\partial}{\partial x} + \frac{A_{55}}{x} + \frac{A_{45}}{xs}\frac{\partial}{\partial\theta}$$

$$L_{35} = \frac{-1}{xt}\left(\frac{B_{22}}{xs}\frac{\partial}{\partial\theta} + B_{26}\left(\frac{\partial}{\partial x} - \frac{1}{x}\right)\right) + A_{45}\frac{\partial}{\partial x} + \frac{A_{45}}{x} + \frac{A_{44}}{xs}\frac{\partial}{\partial\theta}$$

$$L_{41} = \frac{\partial}{\partial x}\left(B_{11}\frac{\partial}{\partial x} + \frac{B_{12}}{x} + \frac{B_{16}}{xs}\frac{\partial}{\partial\theta}\right) + \frac{1}{x}\left(B_{11}\frac{\partial}{\partial x} + \frac{B_{12}}{x} + \frac{B_{16}}{xs}\frac{\partial}{\partial\theta}\right) - \frac{1}{x}\left(B_{12}\frac{\partial}{\partial x} + \frac{B_{22}}{x} + \frac{B_{26}}{xs}\frac{\partial}{\partial\theta}\right) + \frac{1}{xs}\frac{\partial}{\partial\theta}\left(B_{16}\frac{\partial}{\partial x} + \frac{B_{26}}{x} + \frac{B_{66}}{xs}\frac{\partial}{\partial\theta}\right)$$

$$L_{42} = \frac{\partial}{\partial x}\left(\frac{B_{12}}{xs}\frac{\partial}{\partial\theta} + B_{16}\left(\frac{\partial}{\partial x} - \frac{1}{x}\right)\right) + \frac{1}{x}\left(\frac{B_{12}}{xs}\frac{\partial}{\partial\theta} + B_{16}\left(\frac{\partial}{\partial x} - \frac{1}{x}\right)\right) - \frac{1}{x}\left(\frac{B_{22}}{xs}\frac{\partial}{\partial\theta} + B_{26}\left(\frac{\partial}{\partial x} - \frac{1}{x}\right)\right) + \frac{1}{xs}\frac{\partial}{\partial\theta}\left(\frac{B_{26}}{xs}\frac{\partial}{\partial\theta} + B_{66}\left(\frac{\partial}{\partial x} - \frac{1}{x}\right)\right) + \frac{A_{45}}{xt}$$

$$
\begin{aligned}
L_{43} &= \frac{\partial}{\partial x}\left(\frac{B_{12}}{xt}\right) + \frac{1}{x}\left(\frac{B_{12}}{xt}\right) - \frac{1}{x}\left(\frac{B_{22}}{xt}\right) + \frac{1}{xs}\frac{\partial}{\partial\theta}\left(\frac{B_{26}}{xt}\right) \\
&\quad - \left(\frac{A_{45}}{xs}\frac{\partial}{\partial\theta} + A_{55}\frac{\partial}{\partial x}\right) \\
L_{44} &= \frac{\partial}{\partial x}\left(D_{11}\frac{\partial}{\partial x} + \frac{D_{12}}{x} + \frac{D_{16}}{xs}\frac{\partial}{\partial\theta}\right) + \frac{1}{x}\left(D_{11}\frac{\partial}{\partial x} + \frac{D_{12}}{x} + \frac{D_{16}}{xs}\frac{\partial}{\partial\theta}\right) \\
&\quad - \frac{1}{x}\left(D_{12}\frac{\partial}{\partial x} + \frac{D_{22}}{x} + \frac{D_{26}}{xs}\frac{\partial}{\partial\theta}\right) \\
&\quad + \frac{1}{xs}\frac{\partial}{\partial\theta}\left(D_{16}\frac{\partial}{\partial x} + \frac{D_{26}}{x} + \frac{D_{66}}{xs}\frac{\partial}{\partial\theta}\right) - A_{55} \\
L_{45} &= \frac{\partial}{\partial x}\left(\frac{D_{12}}{xs}\frac{\partial}{\partial\theta} + D_{16}\left(\frac{\partial}{\partial x} - \frac{1}{x}\right)\right) + \frac{1}{x}\left(\frac{D_{12}}{xs}\frac{\partial}{\partial\theta} + D_{16}\left(\frac{\partial}{\partial x} - \frac{1}{x}\right)\right) \\
&\quad - \frac{1}{x}\left(\frac{D_{22}}{xs}\frac{\partial}{\partial\theta} + D_{26}\left(\frac{\partial}{\partial x} - \frac{1}{x}\right)\right) \\
&\quad + \frac{1}{xs}\frac{\partial}{\partial\theta}\left(\frac{D_{22}}{xs}\frac{\partial}{\partial\theta} + D_{26}\left(\frac{\partial}{\partial x} - \frac{1}{x}\right)\right) - A_{45} \\
L_{51} &= \frac{1}{xs}\frac{\partial}{\partial\theta}\left(B_{12}\frac{\partial}{\partial x} + \frac{B_{22}}{x} + \frac{B_{26}}{xs}\frac{\partial}{\partial\theta}\right) + \frac{\partial}{\partial x}\left(B_{16}\frac{\partial}{\partial x} + \frac{B_{26}}{x} + \frac{B_{66}}{xs}\frac{\partial}{\partial\theta}\right) \\
&\quad + \frac{2}{x}\left(B_{16}\frac{\partial}{\partial x} + \frac{B_{26}}{x} + \frac{B_{66}}{xs}\frac{\partial}{\partial\theta}\right) \\
L_{52} &= \frac{1}{xs}\frac{\partial}{\partial\theta}\left(\frac{B_{22}}{xs}\frac{\partial}{\partial\theta} + B_{26}\left(\frac{\partial}{\partial x} - \frac{1}{x}\right)\right) + \frac{\partial}{\partial x}\left(\frac{B_{26}}{xs}\frac{\partial}{\partial\theta} + B_{66}\left(\frac{\partial}{\partial x} - \frac{1}{x}\right)\right) \\
&\quad + \frac{2}{x}\left(\frac{B_{26}}{xs}\frac{\partial}{\partial\theta} + B_{66}\left(\frac{\partial}{\partial x} - \frac{1}{x}\right)\right) + \frac{A_{44}}{xt} \\
L_{53} &= \frac{1}{xs}\frac{\partial}{\partial\theta}\left(\frac{B_{22}}{xt}\right) + \frac{\partial}{\partial x}\left(\frac{B_{26}}{xt}\right) + \frac{2B_{26}}{x^2t} - \left(\frac{A_{44}}{xs}\frac{\partial}{\partial\theta} + A_{45}\frac{\partial}{\partial x}\right) \\
L_{54} &= \frac{1}{xs}\frac{\partial}{\partial\theta}\left(D_{12}\frac{\partial}{\partial x} + \frac{D_{22}}{x} + \frac{D_{26}}{xs}\frac{\partial}{\partial\theta}\right) + \frac{\partial}{\partial x}\left(D_{16}\frac{\partial}{\partial x} + \frac{D_{26}}{x} + \frac{D_{66}}{xs}\frac{\partial}{\partial\theta}\right) \\
&\quad + \frac{2}{x}\left(D_{16}\frac{\partial}{\partial x} + \frac{D_{26}}{x} + \frac{D_{66}}{xs}\frac{\partial}{\partial\theta}\right) - A_{45} \\
L_{55} &= \frac{1}{xs}\frac{\partial}{\partial\theta}\left(\frac{D_{22}}{xs}\frac{\partial}{\partial\theta} + D_{26}\left(\frac{\partial}{\partial x} - \frac{1}{x}\right)\right) + \frac{\partial}{\partial x}\left(\frac{D_{26}}{xs}\frac{\partial}{\partial\theta} + D_{66}\left(\frac{\partial}{\partial x} - \frac{1}{x}\right)\right) \\
&\quad + \frac{2}{x}\left(\frac{D_{26}}{xs}\frac{\partial}{\partial\theta} + D_{66}\left(\frac{\partial}{\partial x} - \frac{1}{x}\right)\right) - A_{44}
\end{aligned}
\tag{6.27}
$$

These equations are proven useful when exact solutions are desired.

According to Eqs. (1.60) and (1.61), the general boundary conditions of thick conical shells are:

$$
\begin{aligned}
R = R_0\text{:} &\begin{cases} N_x - k_{x0}^u u = 0 \\ N_{x\theta} - k_{x0}^v v = 0 \\ Q_x - k_{x0}^w w = 0 \\ M_x - K_{x0}^x \phi_x = 0 \\ M_{x\theta} - K_{x0}^\theta \phi_\theta = 0 \end{cases} \qquad
R = R_1\text{:} \begin{cases} N_x + k_{x1}^u u = 0 \\ N_{x\theta} + k_{x1}^v v = 0 \\ Q_x + k_{x1}^w w = 0 \\ M_x + K_{x1}^x \phi_x = 0 \\ M_{x\theta} + K_{x1}^\theta \phi_\theta = 0 \end{cases} \\
\theta = 0\text{:} &\begin{cases} N_{\theta x} - k_{\theta 0}^u u = 0 \\ N_\theta - k_{\theta 0}^v v = 0 \\ Q_\theta - k_{\theta 0}^w w = 0 \\ M_{\theta x} - K_{\theta 0}^x \phi_x = 0 \\ M_\theta - K_{\theta 0}^\theta \phi_\theta = 0 \end{cases} \qquad
\theta = \theta_0\text{:} \begin{cases} N_{\theta x} + k_{\theta 1}^u u = 0 \\ N_\theta + k_{\theta 1}^v v = 0 \\ Q_\theta + k_{\theta 1}^w w = 0 \\ M_{\theta x} + K_{\theta 1}^x \phi_x = 0 \\ M_\theta + K_{\theta 1}^\theta \phi_\theta = 0 \end{cases}
\end{aligned}
\tag{6.28}
$$

Thick conical shells can have up to 24 possible classical boundary conditions at each boundary (see Table 6.2) which leads a high number of combinations of boundary conditions. The classification of the classical boundary conditions shown in Table 1.3 for general thick shells is applicable for thick conical shells.

Table 6.2 shows the importance of developing an accurate, robust and efficient method which is capable of simplifying solution algorithms, reducing model input data and universally dealing with various boundary conditions. This difficulty can be overcome by using the artificial spring boundary technique. In this chapter, we mainly consider four typical boundary conditions which are frequently encountered in practices, i.e., F, SD, S and C boundary conditions. Taking edge $R = R_0$ for example, the corresponding spring rigidities for the four classical boundary conditions are given as in Eq. (5.37).

6.3 Vibration of Laminated Closed Conical Shells

In this section, we consider vibrations of laminated closed conical shells. The open ones will then be treated in the later section of this chapter. It is commonly believed an exact solution is available only for laminated closed conical shells having cross-ply lamination schemes and shear diaphragm boundary conditions at both ends. Tong (1993, 1994a) obtained such solutions for thin and thick conical shells. In this chapter, in the framework of SDST, accurate vibration solutions for laminated conical shells with general boundary conditions, lamination schemes and different geometry parameters will be presented by using the modified Fourier series and weak form solution procedure. For a laminated closed conical shell, there exists two boundaries, i.e., $R = R_0$ and $R = R_1$. Thus, a two-letter string is employed to denote the boundary conditions of the shell, such as F-C identifies the shell with

Table 6.2 Possible classical boundary conditions for thick conical shells at each boundary of R = constant

Boundary type	Conditions
Free boundary conditions	
F	$N_x = N_{x\theta} = Q_x = M_x = M_{x\theta} = 0$
F2	$u = N_{x\theta} = Q_x = M_x = M_{x\theta} = 0$
F3	$N_x = v = Q_x = M_x = M_{x\theta} = 0$
F4	$u = v = Q_x = M_x = M_{x\theta} = 0$
F5	$N_x = N_{x\theta} = Q_x = M_x = \phi_\theta = 0$
F6	$u = N_{x\theta} = Q_x = M_x = \phi_\theta = 0$
F7	$N_x = v = Q_x = M_x = \phi_\theta = 0$
F8	$u = v = Q_x = M_x = \phi_\theta = 0$
Simply supported boundary conditions	
S	$u = v = w = M_x = \phi_\theta = 0$
SD	$N_x = v = w = M_x = \phi_\theta = 0$
S3	$u = N_{x\theta} = w = M_x = \phi_\theta = 0$
S4	$N_x = N_{x\theta} = w = M_x = \phi_\theta = 0$
S5	$u = v = w = M_x = M_{x\theta} = 0$
S6	$N_x = v = w = M_x = M_{x\theta} = 0$
S7	$u = N_{x\theta} = w = M_x = M_{x\theta} = 0$
S8	$N_x = N_{x\theta} = w = M_x = M_{x\theta} = 0$
Clamped boundary conditions	
C	$u = v = w = \phi_x = \phi_\theta = 0$
C2	$N_x = v = w = \phi_x = \phi_\theta = 0$
C3	$u = N_{x\theta} = w = \phi_x = \phi_\theta = 0$
C4	$N_x = N_{x\theta} = w = \phi_x = \phi_\theta = 0$
C5	$u = v = w = \phi_x = M_{x\theta} = 0$
C6	$N_x = v = w = \phi_x = M_{x\theta} = 0$
C7	$u = N_{x\theta} = w = \phi_x = M_{x\theta} = 0$
C8	$N_x = N_{x\theta} = w = \phi_x = M_{x\theta} = 0$

completely free and clamped boundary conditions at the edges $R = R_0$ and $R = R_1$, respectively. Unless otherwise stated, the non-dimensional frequency parameter $\Omega = \omega R_1 \sqrt{\rho h / A_{11}}$ is used in the subsequent analysis and laminated conical shells under consideration are assumed to be composed of composite layers having following material properties: E_2 = 10 GPa, E_1/E_2 = open, μ_{12} = 0.25, $G_{12} = G_{13} = 0.6E_2$, $G_{23} = 0.5E_2$, ρ = 1,500 kg/m^3.

Considering the circumferential symmetry of closed conical shells, each displacement/rotation component of a closed conical shell is expanded as a 1-D modified Fourier series of the following form through Fourier decomposition of the circumferential wave motion:

$$
\begin{aligned}
u(x,\theta) &= \sum_{m=0}^{M}\sum_{n=0}^{N} A_{mn}\cos\lambda_m x\cos n\theta + \sum_{l=1}^{2}\sum_{n=0}^{N} a_{ln}P_l(x)\cos n\theta \\
v(x,\theta) &= \sum_{m=0}^{M}\sum_{n=0}^{N} B_{mn}\cos\lambda_m x\sin n\theta + \sum_{l=1}^{2}\sum_{n=0}^{N} b_{ln}P_l(x)\sin n\theta \\
w(x,\theta) &= \sum_{m=0}^{M}\sum_{n=0}^{N} C_{mn}\cos\lambda_m x\cos n\theta + \sum_{l=1}^{2}\sum_{n=0}^{N} c_{ln}P_l(x)\cos n\theta \\
\phi_x(x,\theta) &= \sum_{m=0}^{M}\sum_{n=0}^{N} D_{mn}\cos\lambda_m x\cos n\theta + \sum_{l=1}^{2}\sum_{n=0}^{N} d_{ln}P_l(x)\cos n\theta \\
\phi_\theta(x,\theta) &= \sum_{m=0}^{M}\sum_{n=0}^{N} E_{mn}\cos\lambda_m x\sin n\theta + \sum_{l=1}^{2}\sum_{n=0}^{N} e_{ln}P_l(x)\sin n\theta
\end{aligned}
\tag{6.29}
$$

where $\lambda_m = m\pi/L$. Similarly, n represents the circumferential wave number of the corresponding mode. It should be note that n is a non-negative integer. Interchanging of sin $n\theta$ and cos $n\theta$ in Eq. (6.29), another set of free vibration modes (anti-symmetric modes) can be obtained. It is obvious that each displacement and rotation component in the FSDT displacement field is required to have up to the second derivatives [see Eq. (6.27)]. Thus, two auxiliary polynomial functions P_l (x) are introduced in each displacement expression to remove all the discontinuities potentially associated with the first-order derivatives at the boundaries. These auxiliary functions are defined as in Eq. (5.39).

6.3.1 Convergence Studies and Result Verification

Table 6.3 shows the convergence study of the natural frequencies (Hz) for a single-layered conical shell with F–F and C–C boundary conditions. The geometric and material constants of the shell are: $R_0 = 1$ m, $L = 2$ m, $h = 0.1$ m, $\varphi = 45°$, $E_1/E_2 = 15$. Five truncation schemes (i.e. $M = 11 - 15$ and $N = 10$) are performed in the study. The table shows the present solutions converge fast. The maximum differences between the '11 × 10' and '15 × 10' form results for the F–F and C–C boundary conditions are less than 0.025 and 0.004 %, respectively. In addition, comparing with Table 5.3, we can find that the convergence of the solutions for the cylindrical shells is better than the conical ones. Furthermore, the C–C solutions converge faster than those of F–F boundary conditions. Unless otherwise stated, the truncated number of the displacement expressions will be uniformly selected as $M = 15$ in the following discussions.

To further validate the accuracy and reliability of current method, the current solutions are compared with those reported by other researchers by the subsequent numerical examples. Table 6.4 lists the comparison of the fundamental dimensionless frequencies Ω for cross-ply conical shells with different boundary

Table 6.3 Convergence of the natural frequencies (Hz) for a single-layered conical shell with F–F and C–C boundary conditions (R_0 = 1 m, L = 2 m, h = 0.1 m, φ = 45°, E_1/E_2 = 15)

B.C.	M	Mode number					
		1	2	3	4	5	6
F–F	11	1.3975	10.045	25.970	40.249	46.792	71.916
	12	1.3972	10.045	25.969	40.243	46.791	71.913
	13	1.3972	10.045	25.969	40.242	46.790	71.913
	14	1.3971	10.045	25.969	40.239	46.790	71.912
	15	1.3971	10.045	25.969	40.239	46.790	71.912
C–C	11	247.80	252.15	253.50	266.46	269.13	281.76
	12	247.80	252.15	253.50	266.47	269.13	281.76
	13	247.80	252.14	253.50	266.46	269.13	281.76
	14	247.80	252.14	253.50	266.46	269.13	281.76
	15	247.79	252.14	253.50	266.45	269.13	281.76

Table 6.4 Comparison of the fundamental frequency parameters Ω for two cross-ply conical shells with various thickness-radius ratios (R_0 = 0.75 m, L = 0.5 m, φ = 30°)

B.C.	Layout	Method	h/R_1				
			0.01	0.03	0.05	0.07	0.09
SD–SD	[0°/90°]	CST (Shu 1996)	0.1799	0.2397	0.2841	0.3277	0.3680
		FSDT (Wu and Lee 2011)	0.1759	0.2320	0.2710	0.3061	0.3358
		Present	0.1759	0.2320	0.2710	0.3061	0.3358
	$[0°/90°]_{10}$	CST (Shu 1996)	0.1976	0.2669	0.3304	0.3873	0.4321
		FSDT (Wu and Lee 2011)	0.1958	0.2607	0.3134	0.3544	0.3832
		Present	0.1958	0.2607	0.3134	0.3544	0.3832
C–C	[0°/90°]	CST (Shu 1996)	0.2986	0.6210	0.9331	1.2344	1.5206
		FSDT (Wu and Lee 2011)	0.3045	0.5834	0.7967	0.9476	1.0457
		Present	0.2966	0.5835	0.7971	0.9480	1.0466
	$[0°/90°]_{10}$	CST (Shu 1996)	0.3771	0.8578	1.3361	1.5730	1.5735
		FSDT (Wu and Lee 2011)	0.3720	0.7509	0.9797	1.1025	1.1759
		Present	0.3720	0.7509	0.9799	1.1031	1.1770

conditions and thickness-to-large edge radius ratios (h/R_1). Two types of lamination schemes, i.e., [0°/90°] and $[0°/90°]_{10}$, are examined. The SD–SD and C–C boundary conditions are considered in the comparisons. The thickness-to-large edge radius ratio h/R_1 is varied from 0.01 to 0.09 by a step of 0.02, corresponding to thin to moderately thick conical shells. The material constants and geometry parameters of the shell are: E_2 = 10 GPa, E_1/E_2 = 15, μ_{12} = 0.25, $G_{12} = 0.5E_2$, $G_{13} = 0.3846E_2$,

Table 6.5 Comparison of the frequency parameters Ω for a cross-ply $[0°/90°]_{10}$ conical shell with various boundary conditions (R_0 = 0.75 m, L = 0.5 m, φ = 30°, m = 1)

n	FSDT (Qu et al. 2013a)			Present		
	S–F	S–S	S–C	S–F	S–S	S–C
0	0.6527	1.2919	1.4065	0.6528	1.2919	1.4065
1	0.4016	1.0903	1.1977	0.4016	1.0903	1.1976
2	0.2711	0.9789	1.1020	0.2712	0.9789	1.1020
3	0.2941	0.9692	1.0945	0.2941	0.9692	1.0944
4	0.4315	1.0312	1.1488	0.4315	1.0312	1.1487
5	0.6203	1.1490	1.2545	0.6203	1.1490	1.2545
6	0.8315	1.3076	1.4007	0.8315	1.3076	1.4006
7	1.0532	1.4936	1.5757	1.0532	1.4936	1.5756
8	1.2796	1.6968	1.7700	1.2796	1.6968	1.7700
9	1.5078	1.9105	1.9768	1.5078	1.9105	1.9767

$G_{23} = 0.3846E_2$, $R_0 = 0.75$ m, $L = 0.5$ m and $\varphi = 30°$. The comparisons are performed between the present results and the FSDT solutions reported by Wu and Lee (2011) and CST solutions published by Shu (1996). The comparisons in the table show a excellent agreement between the present results and those reported by Wu and Lee (2011). It is obvious that the discrepancies are negligible and not exceed 0.012 % for the worst case. The comparisons validate the high accuracy of the modified Fourier series method in predicting vibrations of composite conical shells.

In Table 6.5, the first longitudinal mode (m = 1) frequency parameters Ω for the $[0°/90°]_{10}$ conical shell given in Table 6.4 with three set of classical boundary conditions, i.e., S–F, S–S and S–C are presented. The lowest ten circumference wave numbers (i.e., n = 1–10) are considered in the calculation. The results reported by Qu et al. (2013a) based on the first-order shear deformation theory are also included in the table. A consistent agreement of the present results and the referential data can be seen from the table. The discrepancies are very small and less than 0.015 % for the worst case. The small discrepancies in the results may be attributed to the different solution approaches were used in the literature.

6.3.2 *Laminated Closed Conical Shells with General Boundary Conditions*

Table 6.6 shows the lowest four frequency parameters Ω for a two-layered, [0°/90°] laminated conical shell with various thickness-to-small edge radius ratios (h/R_0). The material properties and geometric constants of the layers of the shell are: E_1/E_2 = 15, R_0 = 1 m, L/R_0 = 2, φ = 45°. Six sets of classical boundary combinations, i.e., F–S, S–F, F–C, C–F, S–S and C–C and five kinds of thickness-to-small edge radius ratios (h/R_0 = 0.01, 0.02, 0.05, 0.1 and 0.15) are included in the table. It can be seen from the

Table 6.6 Frequency parameters Ω for a [0°/90°] laminated conical shell with various boundary conditions and thickness-to-small edge radius ratios (E_1/E_2 = 15, R_0 = 1 m, L/R_0 = 2, φ = 45°)

h/R_0	Mode	Boundary conditions					
		F–S	S–F	F–C	C–F	S–S	C–C
0.01	1	0.1188	0.0415	0.1189	0.0416	0.1364	0.1373
	2	0.1198	0.0454	0.1198	0.0454	0.1399	0.1411
	3	0.1291	0.0455	0.1293	0.0456	0.1417	0.1426
	4	0.1365	0.0546	0.1366	0.0548	0.1527	0.1540
0.02	1	0.1559	0.0543	0.1559	0.0543	0.1786	0.1825
	2	0.1581	0.0613	0.1584	0.0614	0.1802	0.1836
	3	0.1741	0.0620	0.1759	0.0621	0.1961	0.2001
	4	0.1867	0.0775	0.1867	0.0777	0.1977	0.2022
0.05	1	0.2192	0.0754	0.2208	0.0761	0.2538	0.2699
	2	0.2302	0.0914	0.2347	0.0914	0.2728	0.2900
	3	0.2697	0.0922	0.2779	0.0939	0.2766	0.2921
	4	0.2758	0.1268	0.2811	0.1270	0.3256	0.3435
0.10	1	0.2896	0.0988	0.3000	0.1034	0.3408	0.3835
	2	0.2988	0.1061	0.3064	0.1072	0.3746	0.4140
	3	0.3560	0.1584	0.3788	0.1585	0.3862	0.4277
	4	0.4472	0.1585	0.4604	0.1626	0.4593	0.4981
0.15	1	0.3269	0.1070	0.3414	0.1142	0.4197	0.4852
	2	0.3640	0.1396	0.3863	0.1412	0.4300	0.4966
	3	0.4527	0.1595	0.4735	0.1672	0.4992	0.5575
	4	0.4783	0.2249	0.5173	0.2249	0.5760	0.6327

table that the frequency parameters of the shell increase as the thickness-to-small edge radius ratio increases. In addition, it is obviously that the boundary conditions have a conspicuous effect on the vibration frequencies. Increasing the restraint stiffness always results in increments of the frequency parameters.

Table 6.7 lists the lowest four frequency parameters Ω for conical shells with different angle-ply lamination schemes and boundary conditions. Single-layered lamination [0°], antisymmetric laminations [0°/45°] and [0°/45°/0°/45°] and symmetric lamination [0°/45°/0°] are used in the calculation. The geometric and material constants of these shells are: E_1/E_2 = 15, R_0 = 1 m, L/R_0 = 2, h/R_0 = 0.1, φ = 45°. As can be observed from Table 6.7, frequency parameters Ω of the [0°/45°/0°/45°] shell are larger than those of the other three lamination schemes and the minimum frequency parameter for each mode in all the boundary condition occurs at those of single-layered lamination [0°]. In order to enhance our understanding of the vibration behaviors of laminated conical shells, some selected mode shapes and their corresponding frequency parameters $\Omega_{n,m}$ for the [0°/45°/0°/45°] laminated conical shell with F–C boundary condition are plotted in Fig. 6.2, where n and m denote the circumferential wave number and longitudinal mode number. These

Table 6.7 Frequency parameters Ω for laminated conical shells with various lamination schemes and boundary conditions ($E_1/E_2 = 15$, $R_0 = 1$ m, $L/R_0 = 2$, $h/R_0 = 0.1$, $\varphi = 45°$)

Structure element	Mode	Boundary conditions					
		F–S	S–F	F–C	C–F	S–S	C–C
[0°]	1	0.1652	0.0611	0.2024	0.0793	0.2399	0.3751
	2	0.1818	0.0674	0.2143	0.0855	0.2496	0.3817
	3	0.1946	0.0793	0.2366	0.0914	0.2534	0.3837
	4	0.2449	0.1063	0.2766	0.1165	0.2809	0.4033
[0°/45°]	1	0.2890	0.0903	0.3020	0.0972	0.3813	0.4632
	2	0.3219	0.1177	0.3453	0.1219	0.3919	0.4780
	3	0.3612	0.1185	0.3750	0.1254	0.4268	0.5002
	4	0.3995	0.1745	0.4371	0.1762	0.4588	0.5427
[0°/45°/0°]	1	0.2480	0.0898	0.2853	0.1088	0.3389	0.4710
	2	0.2592	0.1016	0.3010	0.1147	0.3476	0.4775
	3	0.3073	0.1150	0.3443	0.1328	0.3623	0.4882
	4	0.3171	0.1380	0.3681	0.1447	0.3873	0.5077
[0°/45°/0°/45°]	1	0.3180	0.1104	0.3427	0.1197	0.4224	0.5190
	2	0.3676	0.1306	0.3977	0.1420	0.4355	0.5270
	3	0.3728	0.1451	0.4013	0.1494	0.4645	0.5582
	4	0.4646	0.2090	0.5102	0.2107	0.4992	0.5814

mode shapes are constructed by means of considering the displacement field in Eq. (6.29) after solving the eigenvalue problem.

The vertex half-angle angle (φ) is a key parameter of a conical shell. The cylindrical shells and annular plates considered in previous chapters can be seen as the special cases of conical shells with zero and 90° ($\pi/2$) vertex half-angle angles, respectively. In the following example, influence of vertex half-angle angle (φ) on the vibration characteristics of laminated conical shells is investigated. Table 6.8 shows the lowest four frequency parameters Ω for a three-layered, cross-ply [0°/90°/0°] conical shell with different boundary conditions. The material constants and geometric parameters are the same as the previous example (see Table 6.7) except that the vertex half-angle angle (φ) of the shell is changed from $\varphi = 15°$ to $\varphi = 75°$ by a step of 15°. The table shows that the shell with C–F and S–F boundary conditions yields lower frequency parameters than those of F–C and F–S boundary conditions. The similar observation can be seen in Tables 6.6 and 6.7. The second observation made here is that the shell with C–F and S–F boundary conditions gave closer results. In addition, we can see that the maximum frequency parameters of the shell with F–S, S–F, F–C, C–F, S–S and C–C boundary conditions occur at $\varphi = 45°$, 15°, 60°, 15°, 45° and 75°, respectively.

Effects of the lamination layer number on the frequency parameters of conical shells are investigated as well. In Fig. 6.3, variation of the lowest three dimensionless frequencies Ω of a $[0°/\vartheta]_n$ layered conical shell with F–C boundary condition against the number of layers n are depicted, respectively (where $n = 1$ means

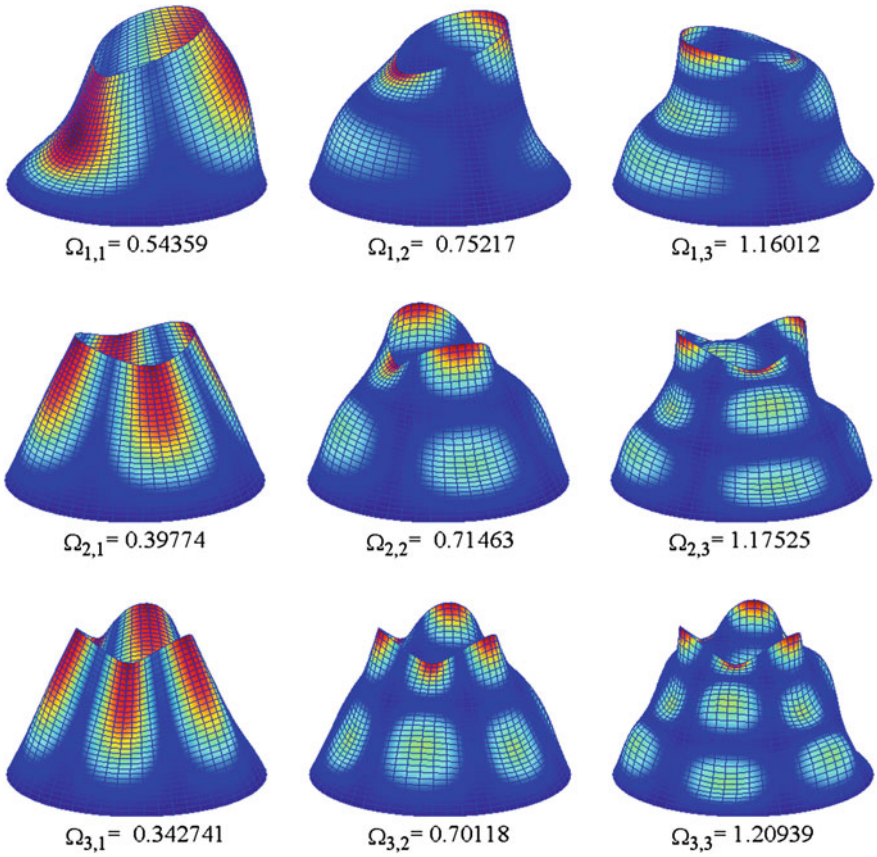

Fig. 6.2 Mode shapes for a [0°/45°/0°/45°] laminated conical shell with F–C boundary condition ($\Omega_{n,m}$, n = 1–3, m = 1–3)

a single-layered shell; $n = 2$ means a two-layered shell, i.e. [0°/ϑ], and so forth). Three lamination schemes, i.e. $\vartheta = 30°$, 45° and 60° are considered in the investigation. The layers of the shells are of equal thickness and made from the same material with follow proprieties: $E_1/E_2 = 15$, $R_0 = 1$ m, $L/R_0 = 2$, $h/R_0 = 0.1$, $\varphi = 45°$. As clearly observed from Fig. 6.3, the frequency parameters of the shell increases rapidly and may reaches their crest around $n = 18$, and beyond this range, the frequency parameters remain unchanged (ignore the fluctuation). The fluctuation on the curves curves curved may be due to the fact that the shell are symmetrically laminated when n is an odd number, and n equal to an even number means the shells are unsymmetrically laminated.

The following numerical analysis is conducted to laminated conical shells with elastic boundary conditions. As what treated in previous chapter, the following two typical uniform elastic boundary conditions are considered in the subsequent analysis (taking edge $R = R_0$ for example):

Table 6.8 Frequency parameters Ω for a [0°/90°/0°] laminated conical shells with different boundary conditions and vertex half-angle angles ($E_1/E_2 = 15$, $R_0 = 1$ m, $L/R_0 = 2$, $h/R_0 = 0.1$)

φ	Mode	Boundary conditions					
		F–S	S–F	F–C	C–F	S–S	C–C
15°	1	0.1504	0.0942	0.1671	0.1051	0.2360	0.3182
	2	0.1582	0.0946	0.1742	0.1087	0.2571	0.3350
	3	0.2094	0.1384	0.2270	0.1434	0.2719	0.3420
	4	0.2466	0.1483	0.2561	0.1568	0.3202	0.3861
30°	1	0.1936	0.0878	0.2226	0.1043	0.2841	0.3996
	2	0.2200	0.0942	0.2455	0.1139	0.2939	0.4078
	3	0.2421	0.1214	0.2761	0.1297	0.3318	0.4310
	4	0.3244	0.1513	0.3630	0.1635	0.3451	0.4474
45°	1	0.2165	0.0791	0.2588	0.1006	0.3066	0.4575
	2	0.2457	0.0843	0.2830	0.1099	0.3159	0.4648
	3	0.2625	0.1092	0.3136	0.1208	0.3506	0.4852
	4	0.3402	0.1394	0.4048	0.1563	0.3628	0.4991
60°	1	0.2131	0.0658	0.2699	0.0931	0.3031	0.4898
	2	0.2226	0.0678	0.2724	0.0970	0.3216	0.5019
	3	0.2683	0.0992	0.3355	0.1132	0.3269	0.5034
	4	0.3414	0.1105	0.3858	0.1332	0.3708	0.5359
75°	1	0.1582	0.0414	0.2200	0.0788	0.2806	0.4994
	2	0.1928	0.0566	0.2612	0.0841	0.2860	0.5026
	3	0.2107	0.0633	0.2626	0.0943	0.3129	0.5179
	4	0.2648	0.0920	0.3442	0.1072	0.3176	0.5213

E^1: the transverse direction is elastically restrained ($w \neq 0$, $u = v = \phi_x = \phi_\theta = 0$), i.e., $k_w = \Gamma$;
E^2: the rotation is elastically restrained ($\phi_x \neq 0$, $u = v = w = \phi_\theta = 0$), i.e., $K_x = \Gamma$

Table 6.9 shows the lowest three frequency parameters Ω of a two-layered [0°/90°] conical shell with different restrain parameters Γ and vertex half-angle angles. The vertex half-angle angle φ varies from 0° to 90° by a step of 30°. The shell parameters used are $E_1/E_2 = 15$, $R_0 = 1$ m, $L/R_0 = 2$, $h/R_0 = 0.05$. The shell is clamped at the edge of $R = R_1$ and with elastic boundary conditions at the other edge. The table shows that when the vertex half-angle angle $\varphi = 0°$, 30° and 60°, increasing restraint rigidities in the transverse and rotation directions have very limited effects on the frequency parameters of the shell. When the restrained rigidity parameter Γ is varied from $10^{-2} \times D$ to $10^4 \times D$, the corresponding maximum differences of the lowest frequency parameters for the shell with E^1–C and E^2–C boundary conditions are less than 1.36, 2.42, 0.85 % and 3.32, 4.45, 1.35 %, respectively. However, the similar frequency parameter differences reach 177, 60, 16 % and 21.4, 22. 3, 18.3 % for the shell with vertex half-angle angle of $\varphi = 90°$.

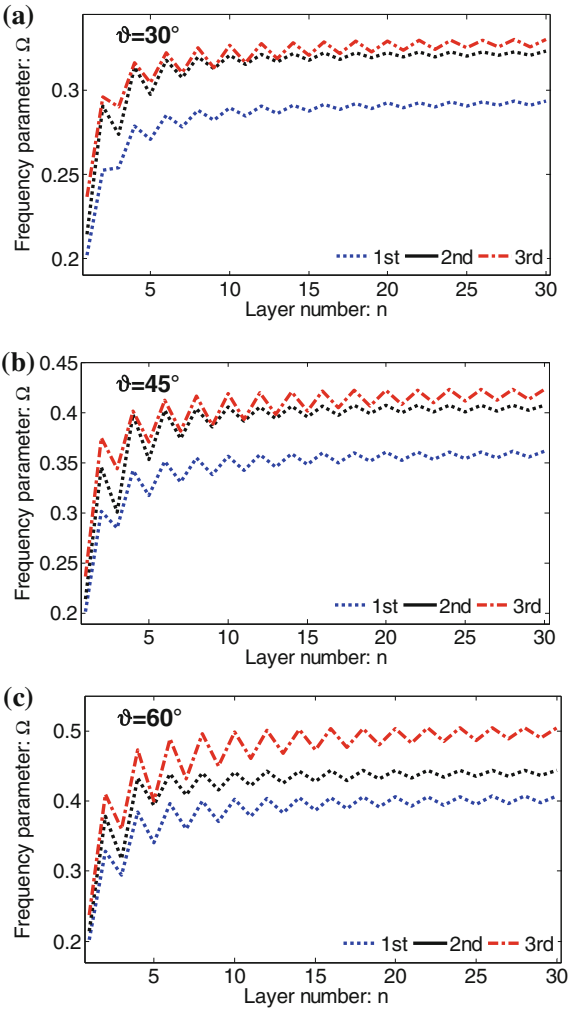

Fig. 6.3 Variation of the frequency parameters Ω versus the number of layers n for a $[0°/\vartheta]_n$ layered conical shell: **a** $\vartheta = 30°$; **b** $\vartheta = 45°$; **c** $\vartheta = 60°$

Table 6.10 shows the similar studies for the shell with F boundary conditions at the edge of $R = R_1$. The table also reveals that when the vertex half-angle angle $\varphi = 0°$, 30° and 60°, increasing the restraint rigidities in the transverse and rotation directions have very limited effects on the frequency parameters of the shell. In addition, it can be seen that the change of the restraint rigidity parameter Γ has large effects on the frequency parameters of all conical shells with vertex half-angle angle $\varphi = 90°$. Increasing the rigidity parameter Γ from $10^{-2} \times D$ to $10^4 \times D$ increases the frequency parameters by almost 651.4, 22.5, 36.5 % and 101.2, 54.6, 94.6 % for the E^1–F and E^2–F boundary conditions, respectively.

Table 6.9 Frequency parameters Ω for a two-layered [0°/90°] conical shell with different restrain parameters Γ and vertex half-angle angles (R_0 = 1 m, L/R_0 = 2, h/R_0 = 0.05, E_1/E_2 = 15)

φ	Γ	E^1–C			E^2–C		
		1	2	3	1	2	3
0°	$10^{-2} \times D$	0.1614	0.1800	0.1960	0.1610	0.1797	0.1955
	$10^{-1} \times D$	0.1614	0.1800	0.1960	0.1610	0.1798	0.1956
	$10^{0} \times D$	0.1614	0.1800	0.1960	0.1616	0.1802	0.1961
	$10^{1} \times D$	0.1615	0.1801	0.1961	0.1627	0.1809	0.1973
	$10^{2} \times D$	0.1619	0.1804	0.1965	0.1630	0.1812	0.1976
	$10^{3} \times D$	0.1627	0.1810	0.1973	0.1631	0.1812	0.1977
	$10^{4} \times D$	0.1630	0.1812	0.1977	0.1631	0.1812	0.1977
30°	$10^{-2} \times D$	0.2555	0.2732	0.2831	0.2533	0.2706	0.2822
	$10^{-1} \times D$	0.2555	0.2732	0.2832	0.2535	0.2708	0.2822
	$10^{0} \times D$	0.2556	0.2732	0.2831	0.2548	0.2726	0.2828
	$10^{1} \times D$	0.2557	0.2734	0.2832	0.2572	0.2760	0.2838
	$10^{2} \times D$	0.2564	0.2745	0.2834	0.2580	0.2771	0.2841
	$10^{3} \times D$	0.2576	0.2765	0.2840	0.2581	0.2772	0.2842
	$10^{4} \times D$	0.2581	0.2771	0.2841	0.2581	0.2772	0.2842
60°	$10^{-2} \times D$	0.2532	0.2577	0.2837	0.2485	0.2527	0.2813
	$10^{-1} \times D$	0.2533	0.2577	0.2838	0.2488	0.2532	0.2815
	$10^{0} \times D$	0.2532	0.2576	0.2839	0.2512	0.2565	0.2825
	$10^{1} \times D$	0.2534	0.2582	0.2834	0.2554	0.2622	0.2845
	$10^{2} \times D$	0.2548	0.2608	0.2843	0.2566	0.2638	0.2851
	$10^{3} \times D$	0.2563	0.2634	0.2850	0.2567	0.2640	0.2851
	$10^{4} \times D$	0.2567	0.2640	0.2851	0.2567	0.2640	0.2851
90°	$10^{-2} \times D$	0.0592	0.1036	0.1434	0.1351	0.1360	0.1406
	$10^{-1} \times D$	0.0614	0.1010	0.1436	0.1370	0.1379	0.1422
	$10^{0} \times D$	0.0793	0.1067	0.1439	0.1476	0.1489	0.1515
	$10^{1} \times D$	0.1364	0.1402	0.1521	0.1607	0.1628	0.1632
	$10^{2} \times D$	0.1608	0.1629	0.1633	0.1636	0.1659	0.1660
	$10^{3} \times D$	0.1637	0.1659	0.1660	0.1640	0.1663	0.1663
	$10^{4} \times D$	0.1640	0.1663	0.1663	0.1640	0.1663	0.1664

6.4 Vibration of Laminated Open Conical Shells

Laminated open conical shells can be obtained by cutting a segment of the laminated closed conical shells. For an open conical shell, the assumption of whole periodic wave numbers in the circumferential direction is inappropriate, and thus, a set of complete two-dimensional analysis is required and resort must be made to a full two-dimensional solution scheme. This forms a major deterrent so that the analyses of deep open conical shells have not been widely available. Among those available, Bardell et al. (1999) studied the vibration of a general three-layer conical

Table 6.10 Frequency parameters Ω for a two-layered [0°/90°] conical shell with different restrain parameters Γ and vertex half-angle angles (R_0 = 1 m, L/R_0 = 2, h/R_0 = 0.05, E_1/E_2 = 15)

φ	Γ	E^1–F			E^2–F		
		1	2	3	1	2	3
0°	$10^{-2} \times D$	0.0904	0.0909	0.1403	0.0909	0.0912	0.1404
	$10^{-1} \times D$	0.0904	0.0909	0.1403	0.0909	0.0912	0.1404
	$10^{0} \times D$	0.0904	0.0909	0.1403	0.0909	0.0912	0.1404
	$10^{1} \times D$	0.0904	0.0909	0.1403	0.0909	0.0912	0.1404
	$10^{2} \times D$	0.0905	0.0910	0.1403	0.0909	0.0912	0.1404
	$10^{3} \times D$	0.0908	0.0912	0.1404	0.0909	0.0912	0.1404
	$10^{4} \times D$	0.0909	0.0912	0.1404	0.0909	0.0912	0.1404
30°	$10^{-2} \times D$	0.0831	0.1018	0.1025	0.0841	0.1027	0.1031
	$10^{-1} \times D$	0.0831	0.1018	0.1025	0.0841	0.1027	0.1031
	$10^{0} \times D$	0.0831	0.1019	0.1025	0.0841	0.1027	0.1033
	$10^{1} \times D$	0.0832	0.1019	0.1025	0.0842	0.1027	0.1037
	$10^{2} \times D$	0.0835	0.1024	0.1026	0.0843	0.1027	0.1038
	$10^{3} \times D$	0.0841	0.1027	0.1034	0.0843	0.1027	0.1038
	$10^{4} \times D$	0.0842	0.1027	0.1037	0.0843	0.1027	0.1038
60°	$10^{-2} \times D$	0.0617	0.0705	0.0801	0.0620	0.0710	0.0803
	$10^{-1} \times D$	0.0617	0.0705	0.0801	0.0620	0.0712	0.0803
	$10^{0} \times D$	0.0617	0.0706	0.0801	0.0625	0.0722	0.0803
	$10^{1} \times D$	0.0618	0.0709	0.0801	0.0631	0.0737	0.0804
	$10^{2} \times D$	0.0625	0.0724	0.0802	0.0632	0.0742	0.0804
	$10^{3} \times D$	0.0631	0.0739	0.0803	0.0633	0.0742	0.0804
	$10^{4} \times D$	0.0632	0.0742	0.0804	0.0633	0.0742	0.0804
90°	$10^{-2} \times D$	0.0030	0.0196	0.0232	0.0110	0.0156	0.0163
	$10^{-1} \times D$	0.0091	0.0197	0.0233	0.0127	0.0172	0.0175
	$10^{0} \times D$	0.0203	0.0224	0.0233	0.0182	0.0208	0.0250
	$10^{1} \times D$	0.0216	0.0236	0.0304	0.0216	0.0235	0.0306
	$10^{2} \times D$	0.0221	0.0240	0.0316	0.0221	0.0240	0.0316
	$10^{3} \times D$	0.0222	0.0240	0.0317	0.0222	0.0240	0.0317
	$10^{4} \times D$	0.0222	0.0240	0.0317	0.0222	0.0240	0.0317

sandwich panel based on the h-p version finite element method. Chern and Chao (2000) made a general survey and comparison for variety of simply supported shallow spherical, cylindrical, plate and saddle panels in rectangular planform. Lee et al. (2002) and Hu et al. (2002) reported the vibration characteristics of twisted cantilevered conical composite shells. Also, vibration of cantilevered laminated composite shallow conical shells was presented by Lim et al. (1998), etc.

In this section, we consider free vibration of laminated deep open conical shells. As was done previously for laminated open cylindrical shells, regardless of boundary conditions, each displacement and rotation component of the open

conical shells under consideration is expanded as a two-dimensional modified Fourier series as Eq. (5.43). The similar non-dimensional parameter $\Omega = \omega R_1\sqrt{\rho h/A_{11}}$ is used in the calculations. And unless otherwise stated, the layers of open conical shells under consideration are made of composite material with following properties: $E_2 = 10$ GPa, $E_1/E_2 =$ open, $\mu_{12} = 0.25$, $G_{12} = G_{13} = G_{23} = 0.5E_2$, $\rho = 1{,}500$ kg/m^3. For an open conical shell, there exits four boundaries, i.e., $R = R_0$, $R = R_1$, $\theta = 0$ and $\theta = \theta_0$. Similarly, the boundary condition of an open conical shell is represented by a four-letter character, such as FCSC identify the shell with F, C, S and C boundary conditions at boundaries $R = R_0$, $\theta = 0$, $R = R_1$ and $\theta = \theta_0$, respectively.

6.4.1 Convergence Studies and Result Verification

Tables 6.11 shows the convergence studies of the lowest six frequency parameters Ω for a three-layered, [0°/90°/0°] deep open conical shell with FFFF and CCCC boundary conditions, respectively. The material and geometry constants of the shell are: $E_1/E_2 = 15$, $R_0 = 1$ m, $L/R_0 = 2$, $h/R_0 = 0.1$, $\varphi = \pi/4$, $\theta_0 = \pi$. The zero frequency parameters corresponding to the rigid body modes of the shell with FFFF boundary conditions are omitted from the results. Excellent convergence of frequencies can be observed in the table. Furthermore, the convergence of the FFFF solutions is faster than those of CCCC boundary conditions.

Table 6.12 shows the comparison of the non-dimensional frequency parameters $\Omega = \omega L^2\sqrt{\rho h/D}$ of SSSS and CCCC supported, [0°/90°/0°] laminated shallow and deep open conical shells with results provided by Ye et al. (2014b) based on the conjunction of Ritz method and the first-order shear deformable shell theory. The

Table 6.11 Convergence of the frequency parameters Ω of a [0°/90°/0°] laminated open conical shell with FFFF and CCCC boundary conditions ($R_0 = 1$ m, $L/R_0 = 2$, $h/R_0 = 0.1$, $\theta_0 = \pi$, $E_1/E_2 = 15$)

B.C.	$M \times N$	Mode number					
		1	2	3	4	5	6
FFFF	14 × 14	0.0181	0.0325	0.0485	0.0711	0.0886	0.1268
	15 × 15	0.0181	0.0325	0.0485	0.0711	0.0885	0.1268
	16 × 16	0.0181	0.0325	0.0485	0.0711	0.0885	0.1268
	17 × 17	0.0181	0.0325	0.0485	0.0711	0.0885	0.1268
	18 × 18	0.0181	0.0325	0.0484	0.0711	0.0885	0.1267
CCCC	14 × 14	0.4588	0.4616	0.5151	0.5259	0.5991	0.6611
	15 × 15	0.4588	0.4615	0.5150	0.5258	0.5987	0.6610
	16 × 16	0.4588	0.4615	0.5149	0.5257	0.5987	0.6602
	17 × 17	0.4588	0.4615	0.5149	0.5257	0.5986	0.6601
	18 × 18	0.4588	0.4615	0.5148	0.5257	0.5986	0.6597

Table 6.12 Comparison of frequency parameters $\Omega = \omega L^2\sqrt{\rho h/D}$ for [0°/90°/0°] laminated shallow and deep open conical shells with SSSS and CCCC boundary conditions (R_0 = 1 m, L/R_0 = 2, h/R_0 = 0.1, φ = π/4, E_1/E_2 = 15)

θ_0	Mode	Ye et al. (2014b)		Present		Difference (%)	
		SSSS	CCCC	SSSS	CCCC	SSSS	CCCC
45°	1	29.953	37.831	29.956	37.831	0.010	0.002
	2	32.542	44.176	32.543	44.177	0.003	0.002
	3	50.005	58.363	50.006	58.364	0.003	0.001
	4	52.410	67.406	52.415	67.408	0.010	0.002
90°	1	16.702	24.103	16.704	24.104	0.012	0.002
	2	19.810	27.671	19.814	27.673	0.019	0.008
	3	29.910	37.898	29.918	37.900	0.027	0.003
	4	33.347	39.299	33.349	39.304	0.005	0.014
135°	1	15.281	22.565	15.284	22.566	0.019	0.004
	2	16.536	22.888	16.537	22.889	0.010	0.004
	3	19.943	26.779	19.949	26.782	0.027	0.010
	4	22.977	30.186	22.989	30.197	0.049	0.035
180°	1	14.820	21.855	14.823	21.856	0.023	0.002
	2	15.129	21.983	15.129	21.985	0.005	0.010
	3	17.444	24.519	17.454	24.525	0.058	0.022
	4	19.367	25.038	19.375	25.042	0.038	0.018
225°	1	14.571	21.526	14.572	21.527	0.006	0.002
	2	14.588	21.667	14.592	21.670	0.028	0.012
	3	16.470	23.078	16.480	23.078	0.065	0.002
	4	16.915	23.431	16.916	23.438	0.003	0.030

shell parameters used in the comparison are the same as those for Table 6.11. Five different circumferential included angles, i.e., θ_0 = 45°, 90°, 135°, 180° and 225°, corresponding to shallow to deep open conical shells are performed in the comparison. It is clearly evident that the present solutions are in a good agreement with the referential data, although different admissible displacement functions were employed by Ye et al. (2014b). The differences between the two results are very small, and do not exceed 0.065 % for the worst case.

6.4.2 *Laminated Open Conical Shells with General Boundary Conditions*

Some further numerical results for laminated open conical shells with different boundary conditions and shell parameters, such as geometric properties, lamination schemes are given in the subsequent discussions.

Isotropic open conical shells are a special case of the laminated ones. Vibration results of these shells with general boundary conditions are rare in the literature as well. Therefore, Table 6.13 shows the first four frequency parameters Ω of an isotropic ($E = 210$ GPa, $\mu_{12} = 0.3$, $\rho = 7{,}800$ kg/m^3) open conical shell with different types of boundary conditions (FFFC, FFCC, FCCC, CCCF, CCFF and CFFF) and thickness-to-small edge radius ratios (h/R_0). The geometry parameters used in the analysis are: $R_0 = 1$ m, $L = 2$ m, $\theta_0 = 90°$, $\varphi = 30°$. Four different thickness-to-small edge radius ratios, i.e., $h/R_0 = 0.01$, 0.02, 0.05 and 0.1 are used in the calculation. The table shows that the frequency parameters of the shell tend to increase with thickness-to-small edge radius ratio increases. This is true due to the stiffness of an isotropic open conical shell increases with thickness increases. Furthermore, it is interesting to find that the frequency parameters of the shell with cantilever boundary conditions in the curved edge are higher than those of straight edges.

The first six mode shapes for the shell with thickness-to-small edge radius ratio $h/R_0 = 0.01$ and FCCC boundary condition are given in Fig. 6.4. These 3-D view mode shapes serve to enhance our understanding of the vibratory characteristics of the open conical shell. Table 6.14 shows the similar studies for a two-layered [0°/90°] open conical shell. The layers of the shell are made of composite material with following properties: $E_1/E_2 = 15$. Table 6.14 also shows that the frequency parameters of laminated open conical shells increase with thickness-to-small edge radius ratio increases.

Table 6.13 Frequency parameters Ω of an isotropic open conical shell with various boundary conditions and thickness-to-radius ratios ($R_0 = 1$ m, $L = 2$ m, $\theta_0 = 90°$, $\varphi = 30°$)

h/R_0	Mode	Boundary conditions					
		FFFC	FFCC	FCCC	CCCF	CCFF	CFFF
0.01	1	0.0037	0.0590	0.2277	0.0996	0.0263	0.0240
	2	0.0100	0.1212	0.2537	0.1907	0.0738	0.0281
	3	0.0172	0.1788	0.3233	0.2479	0.0995	0.0622
	4	0.0345	0.2172	0.3411	0.2769	0.1060	0.0908
0.02	1	0.0074	0.0872	0.3525	0.1501	0.0393	0.0360
	2	0.0198	0.1837	0.3722	0.3004	0.1052	0.0393
	3	0.0342	0.2540	0.4800	0.3473	0.1571	0.1018
	4	0.0681	0.3293	0.5113	0.4079	0.1707	0.1143
0.05	1	0.0184	0.1470	0.5520	0.2695	0.0682	0.0510
	2	0.0489	0.3335	0.6682	0.5239	0.1861	0.0820
	3	0.0842	0.4356	0.8394	0.5964	0.2820	0.1307
	4	0.1629	0.5654	0.9446	0.6877	0.2874	0.2357
0.10	1	0.0366	0.2299	0.8543	0.4357	0.1096	0.0817
	2	0.0953	0.5164	0.9780	0.7747	0.2542	0.1080
	3	0.1652	0.6100	1.2614	0.9499	0.4405	0.2062
	4	0.2996	0.8463	1.2658	1.0000	0.4729	0.4047

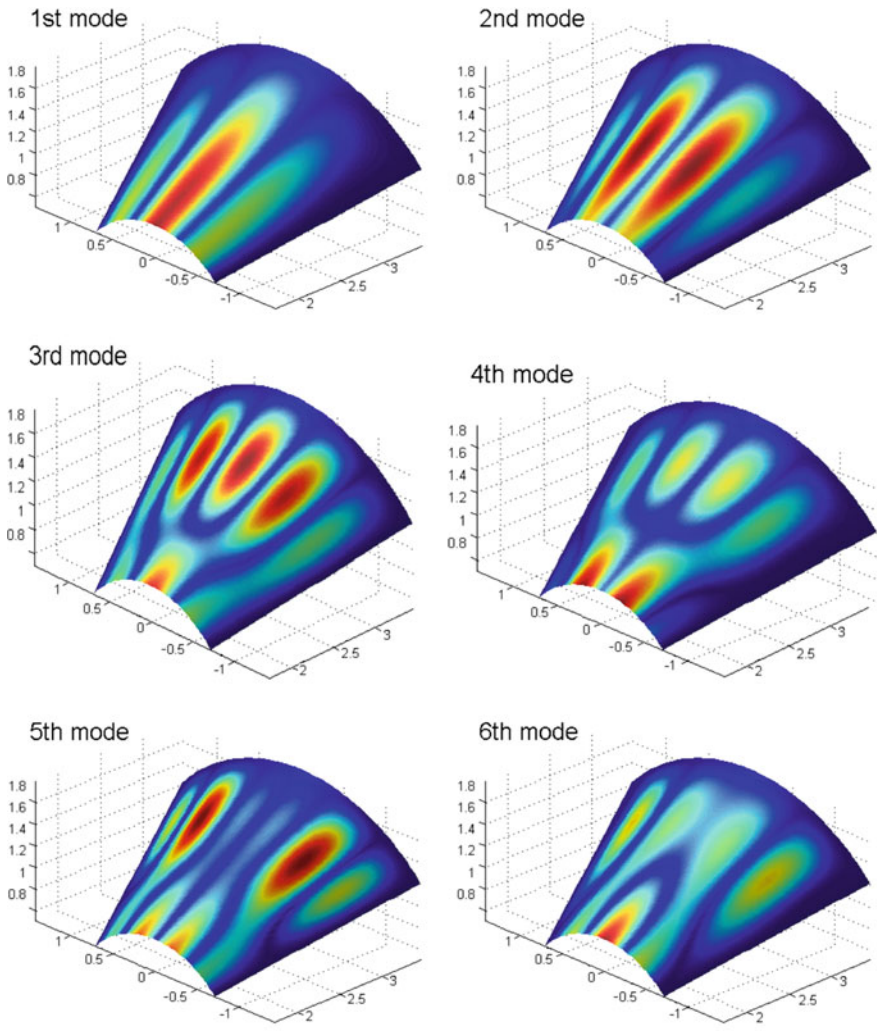

Fig. 6.4 Mode shapes for an isotropic open conical shell with FCCC boundary conditions

Table 6.14 Frequency parameters Ω of a two-layered [0°/90°] open conical shell with various boundary conditions and thickness-to-radius ratios (R_0 = 1 m, L = 2 m, θ_0 = 90°, φ = 30°, E_1/E_2 = 15)

h/R_0	Mode	Boundary conditions					
		FFFC	FFCC	FCCC	CCCF	CCFF	CFFF
0.01	1	0.0024	0.0412	0.1344	0.0628	0.0187	0.0173
	2	0.0052	0.0765	0.1466	0.1147	0.0498	0.0200
	3	0.0102	0.1158	0.1899	0.1394	0.0616	0.0438
	4	0.0202	0.1307	0.1906	0.1556	0.0698	0.0577
0.02	1	0.0047	0.0578	0.1979	0.0906	0.0267	0.0256
	2	0.0102	0.1123	0.2039	0.1760	0.0684	0.0262
	3	0.0201	0.1552	0.2693	0.1926	0.0942	0.0654
	4	0.0399	0.1934	0.2941	0.2173	0.1112	0.0758
0.05	1	0.0118	0.0914	0.3067	0.1583	0.0441	0.0336
	2	0.0254	0.1990	0.3915	0.2830	0.1135	0.0524
	3	0.0491	0.2533	0.4713	0.3519	0.1591	0.0824
	4	0.0953	0.3186	0.5573	0.3917	0.1742	0.1454
0.10	1	0.0234	0.1377	0.4786	0.2556	0.0690	0.0468
	2	0.0498	0.3080	0.6516	0.4231	0.1442	0.0742
	3	0.0946	0.3353	0.6981	0.5271	0.2666	0.1182
	4	0.1735	0.4728	0.8905	0.5919	0.2746	0.2194

At the end of this section, the influence of circumferential included angle θ_0 on the frequency parameters of laminated open conical shells is investigated. A two-layered [0°/90°] open conical shell with small edge radius R_0 = 1 m, length L = 2 m, thickness h = 0.05 m is investigated. The layers of the shell are made of composite material having orthotropy ratio E_1/E_2 = 15. Three different vertex half-angle angles, i.e., φ = 0°, 45° and 90°, corresponding to open cylindrical shell, general open conical shell and sectorial plate are performed in the investigation. Figure 6.5 shows the variation of the lowest three frequency parameters Ω of the shell with SSSS boundary condition against the circumferential included angle θ_0. As observed from the figure, the frequency parameter traces of the shell decline when the circumferential included angle θ_0 is varied from 30° to 330° by a step of 15°. It is attributed to the stiffness of the shell decreases with circumferential included angle θ_0 increases. Furthermore, it is obvious that the effect of the

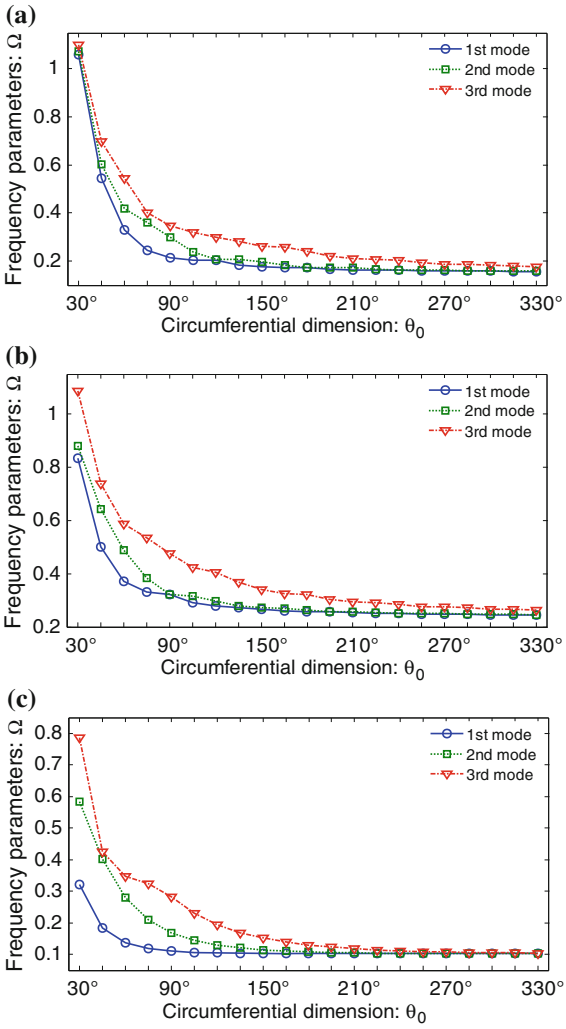

Fig. 6.5 Variation of frequency parameters Ω versus θ_0 for [0°/90°] laminated open conical shells with SSSS boundary condition: **a** $\varphi = 0°$; **b** $\varphi = 45°$; **c** $\varphi = 90°$

circumferential included angle θ_0 is much higher for open cylindrical, conical shells and sectorial plates with lower circumferential included angle. Changing θ_0 from 30° to 90° results in frequency parameters that are more than five times lower. Conversely, increasing θ_0 from 90° to 330° yields less than 30 % decrement of the frequency parameters.

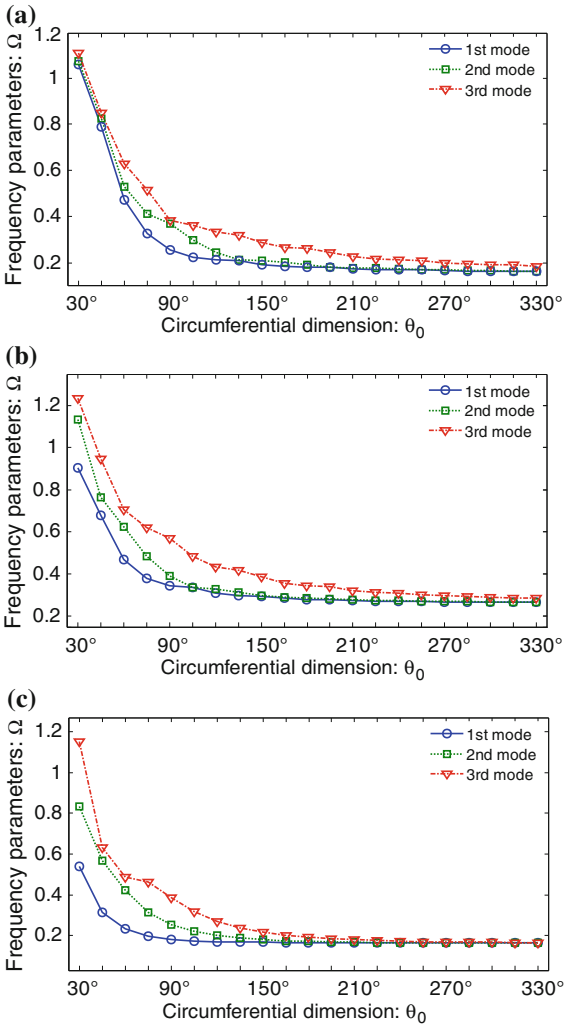

Fig. 6.6 Variation of frequency parameters Ω versus θ_0 for [0°/90°] laminated open conical shells with CCCC boundary condition: **a** $\varphi = 0°$; **b** $\varphi = 45°$; **c** $\varphi = 90°$

Figure 6.6 shows the similar studies for the conical shell with CCCC boundary condition. The similar observations can be seen in this figure.